

Review

# Increasing Thermal Efficiency: Methods, Case Studies, and Integration of Heat Exchangers with Renewable Energy Sources and Heat Pumps for Desalination

Konstantin Osintsev <sup>1</sup>, Sergei Aliukov <sup>2,\*</sup>, Sulpan Kuskarbekova <sup>1</sup>, Tatyana Tarasova <sup>1</sup>, Aleksandr Karelin <sup>1</sup>, Vladimir Konchakov <sup>1</sup> and Olga Kornyakova <sup>1</sup>

- <sup>1</sup> Department of Industrial Thermal Power Engineering, Institute of Energy and Power Engineering, South Ural State University, 76 Prospekt Lenina, 454080 Chelyabinsk, Russia; osintcevk@susu.ru (K.O.); kuskarbekovasi@susu.ru (S.K.); tt9398084@gmail.com (T.T.); karelinasdf@mail.ru (A.K.); vova111002@mail.ru (V.K.); korniakovai@susu.ru (O.K.)
- <sup>2</sup> Department of Automotive Engineering, Institute of Engineering and Technology, South Ural State University, 76 Prospekt Lenina, 454080 Chelyabinsk, Russia
- \* Correspondence: dimaakv@yandex.ru

**Abstract:** The article presents an overview of modern analytical methods and experimental studies on the use of heat exchangers as part of different schemes, as well as technologies that increase the efficiency of heat exchangers using renewable energy sources. The main types of heat exchangers, and the principles of their operation, are considered. In addition, modern technologies for increasing the efficiency of heat exchangers through design are described. The practical experience of using plate heat exchangers in industry has been studied. An overview of the software development that is used in the design and optimization of heat exchange devices, as well as for the improvement of their energy efficiency, is presented. The presented mathematical models can be used for software that is applicable both to individual segments of plates of heat exchangers and heat exchangers in general, taking into account the dependence of the installation of the entire circuit on environmental parameters and location. In conclusion, recommendations are given for further research directions in the field of using heat exchangers with the inclusion of renewable energy sources. The technique of an energy technology complex, including a heat pump, a photovoltaic panel, and a desalination plant, is presented. The methodology is built around the basic design and energy balance of the complex, and it is also considered from the point of view of the exergetic balance. This allows for the use of additional components, such as a turbo expander for the implementation of the organic Rankine cycle, a wind turbine, and a solar concentrator. This scientific approach can become unified for the design and operation of an energy technology complex. In addition, an exergetic calculation method is presented for a thermal desalination plant operating as part of an energy technology complex with renewable energy sources.

**Keywords:** heat exchangers; organic Rankine cycle; renewable energy sources; heat pumps; energy complexes



**Citation:** Osintsev, K.; Aliukov, S.; Kuskarbekova, S.; Tarasova, T.; Karelin, A.; Konchakov, V.; Kornyakova, O. Increasing Thermal Efficiency: Methods, Case Studies, and Integration of Heat Exchangers with Renewable Energy Sources and Heat Pumps for Desalination. *Energies* **2023**, *16*, 4930. <https://doi.org/10.3390/en16134930>

Academic Editors: Fabio Polonara, Sandro Nizetic, Vítor António Ferreira da Costa and Alice Mugnini

Received: 4 May 2023  
Revised: 14 June 2023  
Accepted: 21 June 2023  
Published: 25 June 2023



**Copyright:** © 2023 by the authors. Licensee MDPI, Basel, Switzerland. This article is an open access article distributed under the terms and conditions of the Creative Commons Attribution (CC BY) license (<https://creativecommons.org/licenses/by/4.0/>).

## 1. Introduction

In the field of thermal efficiency, researchers focus on the development of methods and technologies aimed at increasing productivity and energy efficiency, as well as improving systems to achieve a reduction in heat loss. This area of research is particularly relevant in industries such as power generation, heating, ventilation, and air conditioning (HVAC), as well as refrigeration.

The article reviews the literature describing the development of the design of plate heat exchangers in industry, as well as the analytical model and the use of software to optimize the design of heat exchangers of the selected type.

Two case studies are presented demonstrating the application of the developed software and the positive results that can be achieved. In addition, the proposed model and software can be used to optimize heat exchangers and, ultimately, reduce energy consumption.

In general, the field of thermal efficiency improvement covers various research areas, including advanced heat exchangers, waste heat recovery, cogeneration systems, and advanced management strategies. Heat pumps, in particular, open up opportunities for energy-efficient water desalination processes by using external energy sources to produce the necessary heat. Current research aims to further optimize these methods and technologies to improve overall system performance and contribute to sustainable energy solutions [1].

## 2. Literature Review on the Issue

### 2.1. Design Solutions of Heat Exchangers

The article contains information on the numerical study of turbulent flow and heat transfer of capsule-type plate heat exchangers. The influence of length and width parameters on heat transfer and flow characteristics during flow was studied. The proposed heat exchangers were tested in a closed-loop system. The heat-exchange experiment was carried out with a change in the flow rate. To simulate the flow, the ANSYS CFX 16.0 program was used using the SST  $k$ - $\nu$  turbulence model. The computational domain is determined by the boundary conditions of the wall with constant temperature and non-slip velocity; periodic boundary conditions are used in the transverse directions.

The results showed that vortices form in the channels, which contribute to heat transfer and destabilization. As the Reynolds number increases, the trace vortices transform into longitudinal vortices, and as the number of vortices decreases, the size of the vortices increases. In addition, the Nusselt number and the coefficient of friction decrease with an increase in the ratio of the length and width of the capsule. Correlations of the coefficient of friction and the Nusselt number as a function of the Reynolds number, as well as the ratio of the length to the width of the capsule, are obtained. Two different performance evaluations have been conducted to evaluate the comprehensive characteristics of capsule-type plate heat exchangers. It is concluded that such heat exchangers with small length and diameter parameters are recommended for use with the intensive heat transfer of the flow [2].

Various types of spiral heat exchangers and their design features were discussed. The conducted studies were aimed at studying the parameters that affect the efficiency of the selected heat exchangers. The curvature coefficient, spiral pitch, flow rate, and temperature are important factors in the design of spiral heat exchangers. In turn, nanofluids can be effectively used in phase transition materials, as well as shell-and-tube heat exchangers. The addition of nanoparticles to paraffin and water in pipes improves thermal characteristics. However, the use of nanofluids in shell-and-tube heat exchangers increases convective heat transfer and the destruction of exergy. The use of computational fluid dynamics is effective for optimizing the performance of spiral heat exchangers, while numerical modeling has proved useful for predicting the length of spiral-wound heat exchangers. It is concluded that an increase in the diameter of the coil, as well as the mass flow rate, increases the pressure drop. At the same time, the conditions of parallel internal flow provide the highest heat transfer rates [3].

An overview of the advantages of spiral-wound heat exchangers is presented, and their impact on flow and heat transfer performance is discussed. A numerical model was developed to study the influence of five geometric factors on the thermal and hydraulic characteristics of the selected type of heat exchangers. The Taguchi method was used to estimate the contribution coefficients of geometric parameters. The influence of the gap thickness, the pipe pitch in the first layer, the outer diameter of the pipe, the number of layers, and the diameter of the central core on the Nusselt number and pressure drop have been studied. The greater thickness of the dividing strip led to an increase in the volume of the flow channel on the side of the housing but a smaller number of Nusselts and a

decrease in pressure drop per unit length; an increase in the pipe pitch led to a decrease in the number of Nusselts and pressure drop per unit length of the pipe; and an increase in the outer diameter of the pipe led to an increase in the number of Nusselts and pressure drop per unit length in the pipes. The number of layers had a positive effect on the Nusselt number and the pressure drop per unit length of the pipe, while the larger diameter of the central core led to higher Nusselt numbers and pressure drops.

The results of the Taguchi method showed that the number of layers, the diameter of the core, and the outer diameter of the pipe had the greatest contribution. A multidimensional correlation has been developed to accurately estimate the Nusselt number and the coefficient of friction, taking into account the corresponding geometric factors. The unstructured meshes were generated by ANSYS ICEM and enlarged accordingly to obtain more accurate results. The pressure-related algorithm was used to solve control equations, and the SIMPLEC algorithm was used to numerically solve control equations. The results demonstrate that the RNG kee model is the most effective compared to experimental data. The study provides valuable information on ways to optimize the design of the heat exchanger to increase productivity, which is useful for practical application [4].

This article presents software for the design of a spiral-wound heat exchanger with a two-way phase change. The segmented calculation method is used to increase the accuracy of the liquid property parameters when designing the selected type of heat exchangers. The influence of design parameters on the performance of the heat exchanger was also analyzed, which indicates that the ratio of length to diameter affects the heat transfer area and pressure drop. This software can be implemented in the design and calculation of the heat transfer with a phase change in multicomponent mixed systems. The structure of the software is based on the principle and method of designing tubular heat exchangers. The software development results were compared with the actual engineering data, and the error was within the acceptable range.

The diameter of the heat transfer tube has an effect, as well as the diameter of the core, although it does not affect the heat transfer area and the pressure drop from the pipe and shell. The length-to-diameter ratio affects the heat transfer area. As a result, increasing the length-to-diameter ratio can reduce the heat transfer area. At the same time, the length-to-diameter ratio affects the pressure drop on the side of the housing, and an increase in the length-to-diameter ratio may increase the pressure drop on the side of the housing. The physical parameters of the liquid correspond to the average temperature of each segment, which reduces the influence of physical parameters on temperature changes. A comparison between the software design, and the actual technical data showed that the output temperature error was less than 2%, while the pressure drop error was less than 5%.

The uncertainty of the test was calculated with reference to the literature, and it was shown that the results are reliable and accurate. This study provides a theoretical basis for the design and optimization of a spiral-wound heat exchanger, while the design software turns out to be accurate, faster, and more efficient [5].

In addition, this study provides a comprehensive review and analysis of the development and application of double-tube heat exchangers, including methods for increasing the heat transfer rate. Studies of nanofluids in two-tube heat exchangers are discussed, while correlations of the Nusselt number and the differential pressure coefficient are presented. The review shows that methods of improving heat transfer, such as the use of twisted tapes, elongation of the surface, the introduction of wire coils, and other turbulators, can significantly increase the heat-transfer rate and reduce the pressure drop. It has been proven that nanofluids are an effective method of increasing the heat transfer rate that do not present problems with clogging and abrasion. The authors suggest that further efforts should be made to focus on the combination of nanofluids and passive methods of temperature increases [6].

This article presents the results of a study of the thermal characteristics of a two-tube heat exchanger using hybrid nanofluids consisting of aluminum nitride nanoparticles in ethylene glycol. Experiments have shown that the coefficient of friction decreased with

increasing flow velocity and increased with increasing volume concentration of nanofluid, while the Nusselt number increased both with increasing flow velocity and increasing volume concentration. It was determined that the use of hybrid nanofluid significantly improves the thermal characteristics of the heat exchanger. It was also determined that the experimental results are in good agreement with the Darcy–Weisbach and Shah correlations [7].

## 2.2. Applied Methods of Increasing Efficiency

The aim of the work [8] was to study the improvement of heat transfer and pressure loss in the selected apparatus equipped with a perforated turbolentor. A multi-purpose genetic algorithm, a numerical method, and a genetic algorithm for sorting without Dominance-II (NSGA II) were used. The algorithm made it possible to optimize the step ratio, which greatly facilitated the work. An experimental installation for heat transfer analysis was presented, including internal and external tubes, thermocouples, a blower, and a digital differential pressure sensor ST-8920. The procedure for finding the Darcy coefficient and the Nusselt number is also described, as well as how to include a turbulator in this procedure. The use of perforated turbulators leads to an increase in the performance of a two-tube water–air heat exchanger and increases convective heat transfer, but with an increase in pressure drop.

The results showed that pressure losses and the Nusselt number decrease with an increase in the  $k$  coefficient. The authors used ANSYS FLUENT 14 for the numerical simulation of flow in a smooth two-tube heat exchanger. The results obtained show that the efficiency of a gas turbine can be increased. In conclusion, the results of this study show that a perforated circular ring has a significant effect on the type of flow and thermal characteristics in a water–air heat exchanger [8].

The study examines the comparison of the efficiency of using an external magnetic field with  $\text{Fe}_3\text{O}_4$  nanofluid and water in a compact finned heat exchanger to improve heat transfer. The thermophysical properties of the selected nanofluid are discussed with a focus on the specific heat capacity, density, viscosity, and thermal conductivity, as well as their dependence on temperature. The results show that the maximum increase in heat transfer was obtained by using magnetite nanoparticles in deionized water as a coolant.

The study provides evidence that the use of an external magnetic field at low Reynolds numbers is more effective than other available methods, since the power of the injection device is not required to increase the mass flow rate. CFD modeling is based on a structured and homogeneous grid with points grouped near the wall and is discretized using a second-order downwind scheme combined with a simple algorithm. An increase in the number of nodes does not lead to an increase in accuracy; it leads to excessive calculation time without additional benefit. The accuracy and reliability of the numerical model used is demonstrated by comparing the numerical results with the experimental ones, with a relative difference between the numerical and experimental results of other scientists.

The approach is one of the possible solutions to the problem of improving heat transfer in equipment designed for limited space and low Reynolds numbers [9].

A comprehensive solution to the problem of increasing the efficiency of heat exchangers in thermal power plants through the use of multi-section heat exchangers is presented. The criteria for evaluating the efficiency of the selected heat exchangers are described. An assessment of local and global criteria, such as cycle cost, energy efficiency, thermal efficiency, and electricity consumption, is compared with payback periods. The analysis of the regenerating section of the two-section waste processing equipment was carried out in the temperature range. The analysis demonstrated that an increase in temperature is impractical due to increased costs. The use of multi-stage heat transfers provides significant cost savings compared to more traditional approaches. Conducting further research on the implementation of such heat transfer processes is proposed. The conclusions of this article can be useful for reducing energy and material costs, as well as for improving the efficiency of thermal power plants [10].

A complex mathematical model of a geothermal heat pump system is presented to assess the temperature fields responsible for the heat exchange process. The results of this model, combined with knowledge of the soil parameters and the geothermal heat pump, are of great importance for determining the appropriate layout of the soil-exchange array and preventing system failure due to soil freezing. The article discusses the main elements of vertical ground heat exchangers used in geothermal heat pumps. Based on structural analysis and further studies of heat transfer and temperature field formation, the authors concluded that vertical ground heat exchangers are preferable for the reliable supply of low-potential energy to ensure the reliable operation of geothermal heat pumps. The use of vertical ground heat exchangers for geothermal heat pumps can play a crucial role in improving energy efficiency and environmental ecology. An overview of the simulation procedure for calculating the temperature field of a ground-based heat exchanger (GHE) is presented. Modeling is based on solving the differential equation of thermal conductivity and requires simplifications to create an approximate mathematical model. The finite element method was used to solve the one-dimensional differential equation of thermal conductivity. The method proposed by E. Shubin is a reasonable approach to carrying out calculations while taking into account the nominal resistance, which preliminarily calculates the heat flow for each pipe involved in mutual influence. This article discusses the impact of a ground-based heat exchanger made of plastic pipes on two sections of the well. The study proved the effectiveness of the GHE design, which has significant implications for the energy efficiency of buildings [11].

The article presents the optimization of shell-and-tube heat exchangers using differential evolution (DE) and a new variant of DE (Tsallis Differential Evolution) to minimize total annual costs. Mathematical models were used to solve the optimization problem. The article also provides background information on the two algorithms used.

The optimization was carried out using three variables (the inner diameter of the housing, the outer diameter of the pipe, and the distance between the partitions) and demonstrated a significant reduction in total annual costs compared to literary methods, the genetic algorithm, particle swarm optimization, biogeography-based optimization, and the cuckoo search algorithm. The best, worst, average, and standard deviations of the cost function were also presented for both algorithms. The results obtained using the DE algorithms and the new DE variant were compared with the results of other studies demonstrating the effectiveness of algorithms for optimizing shell-and-tube heat exchangers.

The results demonstrate the effectiveness of using wide search distributions to adjust the control parameters of evolutionary algorithms, while future work is focused on further improving the solution of heat exchanger problems in the design of a large number of objects and self-tuning control parameters [12].

A new method for determining the variable operating modes of heat exchangers with a tied heat supply is presented. In the method of determining the number of transfer units, constant dimension-less parameters are used, which significantly reduce the number of variables for calculating the parameters of the heat exchanger. This method was used to determine the thermal power, temperature difference, and total flow of mains water between all stages of the heater, as well as groups of heat exchangers with the redistribution of heat flows in variable operation mode. In addition, the method was used to calculate the thermal power of the heating system and change the thermal power of the heat exchanger for the operation of the hot water system. A number of formulas were used to determine the flow rate of mains water, as well as the temperature of heated water. The analysis of the heating point with variable parameters of the I and II stages of the heaters, as well as the corresponding approximations, are presented. Equations and exponential expressions were used to calculate the product of the heat transfer coefficient by area, heat output of the I stage, and temperature differences in the heaters of the I and II stages. The proposed approach proved successful in accurately predicting the flow and temperature of mains water in the heating system and setting up programmable controllers with minimal calculations. This method can be used to improve the configurations of programmable

regulators and optimize the performance of the heating system. The method provides a reliable and efficient approach to the calculation of variable operating modes of heat exchangers with a tied heat supply [13].

The study demonstrated the effectiveness of heat pump technology in providing energy. An in-depth study of heat exchange processes in vertically arranged heat exchangers is carried out using the experimental method and the Temp Keeper program. This allowed for the monitoring and control of temperature and moisture content. Experiments have shown that the temperature distribution around the U-shaped ground heat exchanger varies depending on the moisture content in the sand. When heat is removed, the ground temperature around the ground-heat exchanger decreases. Dependency graphs were also constructed showing the temperature difference with different moisture contents. The results of the experiments can be used to improve energy efficiency and reduce greenhouse gas emissions. The authors conclude that the soil of the surface layers of the Earth is an unlimited heat accumulator [14].

### 2.3. Advantages of the Organic Rankine Cycle

The following article discusses the potential of organic Rankine cycle (CRO) systems for the use of high-temperature heat sources and the effect of an increase in operating temperature on efficiency. Turboden S.p.A.'s research and development have concluded that more high-performance solutions can be obtained through the appropriate choice of fluids. The main areas of the application of CRO systems for biomass, waste to energy, heat recovery, and solar thermal energy are considered. The authors pay special attention to two families of compounds as working fluids: linear hydrocarbons, and aromatic hydrocarbons and their derivatives, as well as a diphenyl oxide–diphenyl mixture. It also describes the possibility of choosing between buying electricity from the grid and producing steam from a boiler or a CHP plant to use a single fuel source, such as natural gas. Comparison of the OVT-CRS with traditional SCR, piston engines, gas turbines, and SRC back pressure technologies indicates a net improvement in electrical performance compared to the best available VT CRS system. In addition, a comparison of CHP technologies and the Steam and Power CRO (ST and P) system suggests that for the ratio of heat to process power, the W CRO (ST and P) technology is the most profitable CHP technology. This highlights the potential of the CRO technology to offer effective solutions for high-temperature thermal power plants with achievable efficiency. Depending on the ratio of heat to process power, different CHP technologies can provide different ways to meet the energy needs of a given production facility. This study estimates capital and operating costs, as well as the savings on electricity costs. The results of this feasibility study show that the technology of high-temperature CRO (ST and P) is the most profitable. Thus, it is concluded that compliance with the technological requirements of a suitable CHP technology can increase the profitability of the system with a significant increase in energy efficiency. In addition, Rankine organic cycle technology can increase the maximum operating temperature when using thermally stable and appropriate fluids. In conclusion, the potential of the CRO technology to provide effective solutions for high-temperature thermal power plants with achievable efficiency and profitability is demonstrated. Therefore, it is assumed that such a technology can be adopted for the operation of both medium- and high-temperature (CT and W) heat sources, and it can provide a competitive advantage in the market [15].

A comparison and evaluation of the performance of three systems of the Rankine CHPP organic cycle is presented: sequential (PS), condensing (SC), and hybrid (PS/SC). Using a genetic algorithm as an optimization method, the system characteristics of three systems in different operating conditions were investigated and compared. The algorithm was also used to optimize the system performance in terms of the maximum return on investment (KPI). The results showed that PS/SC had the highest KPI value. The optimal KPI value for the three CRO–CHP systems increased with an increase in the temperature of the heat source. The exergetic failures of each component and system were calculated and discussed. The analysis showed that most of the exergetic destruction occurred in

the PS and PS/SC systems. All systems showed low electrical efficiency and high thermal efficiency. The economic efficiency of the systems was evaluated, and the applicability of each was considered in the system integration method. The electrical efficiency of the PS decreased and increased, and the thermal efficiency of the PS and PS/SC reached more than 99%. Economic analysis has shown that the cost of heat exchangers accounts for the largest share in all systems. The error in calculating the program was kept within 50%. The above-mentioned comparison and analysis of the thermal economy of various systems of the Rankine organic cycle serve as a guideline for choosing the most suitable system under actual operating conditions. Future work should focus on the economic and thermal optimization of the system to meet broader demand, as well as on conducting appropriate experimental studies [16].

This text presents a comparative analysis on the economic and energy efficiency of a waste heat recovery system (ROT) operating with an organic Rankine cycle (CRO) to reduce carbon dioxide emissions from a natural gas engine. Thermodynamic parameters and operating conditions, such as the temperature and condensation pressure coefficient, are taken into account to determine the optimal fluid. The laws of mass and energy conservation are an important basis for the design of an ROTA to maximize its efficiency. Exergetic analysis was used to measure the destruction of exergy. It provided reliable data for system optimization. Advanced exergetic analysis has shown that components such as the pump and turbine have the greatest potential for improvement with endogenous destruction. To calculate the total production costs of the Rankine regenerative organic cycle system, a thermo-economic analysis was used, while the main resource was the purchase of the necessary equipment to assess the total investment costs. Changing the pump pressure coefficient increased the investment costs for acetone and toluene, while for heptane, the costs decreased with each increase in pressure. In addition, the change in condensation temperature had a significant impact on investment costs, with toluene representing the highest costs in most cases. Increasing the evaporation temperature of the evaporator increased investment costs while reducing energy destruction. A methodology of secondary CRO systems with indirect evaporation is proposed to supply the necessary energy without problems with back pressure to the engine. The economic impact and financial viability of such CRO systems were evaluated in order to determine the cost-effective thermal design of the ROTH. Thermo-economic optimization is vital to provide more cost-effective energy solutions and reduce carbon dioxide emissions. The results of this analysis were applied to other engines. They provided opinions on the development of economically viable solutions to reduce carbon dioxide emissions. The use of extended exergetic analysis as an efficiency indicator is important for a better understanding of the efficiency of recovery of selected heat working with CRS and maximizing their efficiency. This study provides valuable information for expanding the use of renewable energy sources and improving the efficiency of the system, leading to a more sustainable future [17].

This article presents an analysis of the process of selecting working fluids in the organic Rankine cycle (OCR). In the selection process, the authors take into account various criteria, including thermodynamic characteristics, the presence of a regenerator, environmental characteristics, safety, and cost. According to research, liquids such as HFE7100, HFE7000, PF5050, R123, n-Pentane, R-245fa, R134a, and isobutene are suitable for CRO systems. Other fundamental criteria for the successful selection of suitable working fluids for CRO systems are the optimization of the boiling point, evaluation of the useful output power, and consideration of the source temperature relative to the available heat source. The study also discusses an example of choosing a liquid for a CRO system with a useful output power, taking into account such criteria as thermodynamic characteristics, safety, environmental impact, efficiency, and thermal stability. The most suitable liquids for the power plant under discussion were toluene, DMC, and MM. Each has its own advantages and disadvantages. The analysis of this study is useful for understanding that when choosing a working fluid for a CRO system, a careful approach is needed to ensure an optimal balance between performance, safety, cost-effectiveness, and environmental impact.

The potential of the CRO system for heat recovery from a compressor system driven by a gas engine stored in a tank and running on mine gas is also being studied. The exhaust gas temperature of the internal combustion engine ranges from 230.8 °C to 706 °C, and the maximum efficiency of the combined system can increase up to 40%. To carry out the calculations presented in the study, the Matlab program and the NIST Refprop interface are used, which makes it possible to determine the most suitable working fluids for the CRO system under study. Twenty-five different liquids were considered and compared, the most promising of which were toluene, dimethyl carbonate, and hexamethyldisiloxane. Thus, a quantitative assessment of the characteristics, efficiency, and safety of these liquids is carried out. Ultimately, it is concluded that toluene, DMC, and MM are suitable working fluids for a heat recovery system using a CRO for a compressor unit driven by a gas engine. This study demonstrates the importance of choosing the right working fluid for a CRO system in order to maximize efficiency and minimize health hazards. To ensure an optimal balance between performance, safety, cost-effectiveness, and environmental impact, a careful approach is necessary when choosing the working fluid for the CRO system. Based on the evaluation of various fluids and comparison of their characteristics, safety, and environmental impact, the authors determined that toluene, DMC, and MM are the most suitable working fluids for the CRO system [18].

The study presents a new thermo-economic performance indicator, the maximum power factor (MCM) for a waste heat power system. The optimization of the Organic Rankine Cycle (OCR) and Rankine Steam Cycle (PCR) system to maximize the useful output power with a limitation of the Cost of Electricity Production (SPE)  $\leq$  SPE0 is carried out using the genetic algorithm of non-dominant sorting II (NSGA-II). The results show that the microns are greater for the CRO system than for the PCR system, and the thermal and economic characteristics of the two systems are compared using the map selection function for optimal conditions. Energy analysis is based on the first law of thermodynamics, and economic indicators are estimated by the total costs of designing, building, installing a heat recovery system, operating and maintenance costs, annual operating time with full load, and the capital return coefficient. The efficiency of a multi-stage axial turbine used in a PCR system is determined by a number of parameters, such as the nominal power and speed of the turbine, pressure, steam overheating at the inlet, and the turbine load factor, while the efficiency of a three-stage turbine used in a CRO system is estimated based on a numerical equation. The design of the heat exchanger, including the choice of type, size, materials, and layout, also takes into account that finned, shell-and-tube and plate heat exchangers are selected for the heat exchanger, condenser, and regenerator, respectively. The cost of CRO and PCR systems is estimated using the Aspen Process Economic Analyzer (version 9), while the total cost of the system includes direct and indirect costs, such as material and labor costs, design and maintenance costs, and freight and taxes, as well as startup costs. Genetic algorithms (GA) and genetic sorting algorithm without dominance-II (NSGA-II) are used to optimize the system in order to maximize net power output at minimum cost of electricity generation (SPE). The choice of the working fluid for the CRO system depends on the temperature of the heat source, as well as on such characteristics as low GWP and non-combustibility, non-aggressiveness, and non-toxicity. The results of thermo-economic optimization represent a compromise between the goals of achieving a minimum SPE and maximum useful output power, while the CRO system using cyclopentane generates higher microns than the PCR system. The minimum SPEs of PCR and ORC systems depend on the temperature of the heat source, while lower temperatures lead to higher SPEs. The minimum temperature for PCR and cyclopentane-RC systems is 345 °C and 330 °C, respectively. Pareto boundaries show that the CRO system is preferable to PCR for heat source conditions in Region C, while PCR is recommended in Region D. The external costs of coal-fired power plants, such as CO<sub>2</sub> capture and storage, as well as emissions of pollutants into the atmosphere, can further affect the choice map of the CRO or PCR system. This study can be used as a guide for choosing optimal conditions for the use of waste heat in the power system in terms of maximum useful output power and minimum costs [19].

In the mentioned study, genetic algorithms (GA) and the non-dominance-II genetic sorting algorithm (NSGA-II) were used to optimize three different systems under different operating conditions. The goal was to achieve the maximum return on investment represented by the Key Performance Indicator (KPI) of minimizing the cost of electricity generation (SPE) while maximizing the useful output power.

Genetic algorithms were used in the optimization process:

The optimization task was defined in order to maximize the useful output power while maintaining the restriction on the retention of the cost of electricity production (SPE) below the specified threshold value (SPE0). This task was formulated as a multi-purpose optimization problem, since there are many conflicting goals.

Genetic Algorithm (GA): GA is a metaheuristic optimization method inspired by the process of natural selection. It works on the basis of the concept of the evolution of a set of potential solutions through iterations to obtain optimal or close-to-optimal solutions. GA consists of the following stages:

- a. Initialization.
- b. Fitness assessment.
- c. Selection.
- d. Crossing.
- e. Mutation.
- f. Substitution.
- g. Completion.

Genetic Sorting Algorithm without Dominance-II (NSGA-II): NSGA-II is an extension of the basic GA, which is specifically designed for multi-purpose optimization problems. It aims to identify a set of solutions that represent a compromise between conflicting goals, known as the Pareto optimal front. NSGA-II includes the concept of non-dominance, in which a solution is considered better than another if it improves at least one goal without impairing any other goal.

The NSGA-II algorithm performs a sorting procedure to rank solutions based on their non-dominance. This divides the population into various non-dominant fronts, where solutions on the first front are the best in terms of non-dominance. After sorting, the stages of selection, crossing, mutation, and replacement are applied to create the next generation of solutions.

Optimization process: The optimization process using genetic algorithms involved iterative application of GA and NSGA-II algorithms to three different systems under different operating conditions. Design parameters, such as turbine parameters, heat exchanger configuration, and the choice of working fluid, were encoded in the form of chromosomes. The suitability assessment included thermodynamic and economic indicators, such as useful power output and total costs.

Evolving a set of solutions over several generations, genetic algorithms investigated the space of design parameters and determined a set of Pareto optimal solutions. These solutions represented the best compromise between the conflicting goals of maximizing the useful output power and minimizing the cost of electricity production.

The study presents the methodology of energy and exergetic modeling of an internal combustion engine (ICE) on natural gas using the organic Rankine cycle (CRO) and additional cycles of waste heat recovery. The model was tested by comparing the results obtained with the theoretical values given in the literature. The exergetic efficiency of the turbine was about 21.6%, and the efficiency of the pump was about 14.7. The exergetic efficiency of the condenser was about 30.8%, and the exergetic efficiency of the evaporator was about 34.3%. The exergetic efficiency of the recuperator was about 39.4%, and the total exergetic efficiency of the system was about 14.75%. The improvement in the thermal efficiency of the system was about 6.8%, and the total specific reduction in fuel consumption was about 8.2%. An economic analysis of the system showed that the total cost of production was about USD 1914.73 per kilowatt hour. The authors conducted a parametric study of the influence of the degree of pressure increase, condensation temperature, and the tempera-

ture of the pinching point of the evaporator on thermal and exergetic parameters, as well as the operating mode of the thermal system. The useful output power, thermal and exergetic efficiency can be improved by optimizing the operating parameters of the CRO system. The criteria for selecting liquids in CRO systems were discussed, such as the maximum system temperature, molecular weight, boiling point, and pressure, as well as the positive slope in the T–S diagram. Organic liquids with critical temperatures and pressures above 175 °C and from 0.2 to 4 MPa, respectively, were identified as suitable options. Refrigerants such as R123, HFE700, R227ea, and R245FA, as well as hydrocarbons such as pentanes, butanes, octanes, and hexanes, have also been identified as potential working fluids. Advanced exergetic analysis is used to calculate the total exergetic destruction by component, which has been divided into four parts: endogenous, exogenous, preventable, and unavoidable. The results of the energy and exergetic analysis of the CRO system showed that the thermal efficiency of the system increases, and the exergetic destruction is mainly concentrated on the evaporator, regenerator, and condenser. The economic evaluation of the selective heat recovery system using CRO showed that when using pentane as a working fluid, the total production costs amount to USD 9606.56/kW [20].

This article evaluates the possibility of generating electricity from an organic Rankine cycle (OCR) built into a natural gas engine. The operational and design variables that most affect the energy, economic, and environmental performance of the system were thoroughly analyzed. The evaporation pressure had the most significant effect on the destruction of exergy, while the highest proportion of exergy was obtained for the shell-and-tube heat exchanger (ITC1). Increasing the heat transfer area increases the cost and the normalized cost of energy (NSE) of the system. A life cycle analysis (LCA) was performed for a system running on acetone as an organic working fluid. The greatest environmental impact was observed from the turbine. Rankine Organic Cycle Technology (OCR) is an efficient way to convert medium and low temperature heat into electricity. Life cycle analysis (LCA) was used to assess the impact of CRO systems on the environment, emphasizing that the greatest potential impact occurs during the construction phase. Exergetic and economic indicators were used to determine the performance of CRO systems, providing guidance on their application in power generation. In thermodynamic analysis, the effect of destroyed exergy and useful power was studied, as well as a life cycle analysis to demonstrate the effectiveness of the waste heat recovery system of the CRO. The results showed that the pressure of the evaporator affects the exergetic losses and the increase in useful power depending on the evaporation pressure, condensation temperature, the pinching point of the evaporator, and the efficiency of the turbine. The normalized cost of energy (NSE) decreased as the parameters increased. Life cycle analysis has shown that most of the exergetic destruction is concentrated in heat exchangers, with thermal oil being the most important environmental impact factor. This study concluded that direct evaporation of organic liquid with engine exhaust gases should be used to ensure maximum environmental sustainability. To optimize the characteristics of the CRO technology, it is necessary to conduct further studies to study the environmental impact and the choice of effective working fluids [21].

A comprehensive study of the thermodynamic, exergetic, and environmental aspects of the proposed combination of the supercritical Brayton cycle running on carbon dioxide, and the organic Rankine cycle as the lower cycle, is presented. The above analyses are aimed at optimizing the system, which in turn leads to an increase in energy consumption efficiency and a reduction in emissions. The study uses toluene, cyclohexane, and acetone as working fluids and applies a life cycle analysis methodology to assess the environmental impact of the system. A thermodynamic analysis of the combined cycle showed the maximum thermal efficiency for acetone as a working fluid. Meanwhile exergy analysis showed that the components with the greatest exergy destruction and environmental impact were the main and secondary turbines of the Brayton cycle S-CO<sub>2</sub> and ITC1 CRO, respectively. In order to increase the overall energy and exergetic efficiency of the system, it is important to reduce exergetic destruction in these key components. The main turbine (T1) and the

secondary turbine (T2) of the Brayton S-CO<sub>2</sub> cycle have the highest energy and environmental efficiency. The heat exchanger (ITC1) in the ORC cycle has the greatest impact on the environment. Thermal oil also has a significant impact on the environment compared to other organic liquids. In turn, acetone had the greatest impact on the environment of the studied organic liquids. The conclusion reached by the authors: the integrated Brayton S-CO<sub>2</sub>-CR system provides high thermal and energy efficiency, as well as low environmental impact. The system is a promising option for sustainable energy production. It may be useful to further study alternative organic working fluids that have a comparative or lesser impact on the environment. The study provides valuable information about the efficiency and environmental characteristics of the Brayton S-CO<sub>2</sub>-CRO system, which makes it a suitable option for sustainable energy production [22].

#### *2.4. The Use of Exergetic Methods of Thermodynamic Analysis for the Organic Rankine Cycle*

This article discusses the concepts and practices of thermal efficiency, a metric used to evaluate the output of energy to the input data to the system, by providing quantitative data and clarifying the concept with a definition. It is argued that thermal efficiency alone is an insufficient measure to assess the energy efficiency of distributed combined cooling systems for heating and power supply (trigeneration), since it does not take into account the quality changes that occur during energy conversion. The concept of exergy is also considered, which represents the maximum amount of useful work within the system and explores its relationship with the first and second laws of thermodynamics. The relevance of the efficiency of exergy as the main indicator in load analysis is discussed, since it takes into account the ratio of the nonequivalence of cooling or heating energy for operation, while indicators based solely on the first law of thermodynamics cannot represent the influence of the external environment on the sources of the system. In addition, a case study is presented to compare the thermal and exergy efficiency of two types of steam boilers. The results of this study showed that while high thermal efficiency may not necessarily correlate with high operational efficiency, low operational efficiency may still represent significant energy losses. Thus, this article confirms the importance of considering the efficiency of using exergy to accurately assess energy efficiency and productivity, as well as the need to achieve energy savings by avoiding the transition from high-quality to low-grade energy. Efforts to evaluate energy systems should take into account both thermal and exergetic efficiency in order to determine the potential applications and limitations of various types of thermal equipment and sources. Therefore, a comprehensive assessment of energy systems should include this comparison of the two types of efficiency. In addition, efforts should be made to improve energy efficiency in order to reduce irreversible losses arising from energy conversion. The study assessed thermal and exergetic efficiency and, thus, demonstrated their usefulness in understanding the energy efficiency of distributed trigeneration systems. The importance of taking into account not only the amount of energy, but also the quality of energy when measuring energy efficiency is also emphasized. In addition, the critical role of exergetic analysis in energy systems was emphasized, since it is more accurate, comprehensive, and relevant than the effectiveness of the first law. Exergetic efficiency of work is important for assessing the degree of irreversibility of processes and understanding the influence of the external environment. In summary, when evaluating sources and processes that interact with the external environment, an analysis of external factors should be taken in order to increase energy efficiency and productivity [23].

This study examines the use of exergetic analysis for energy systems as a way to reduce losses and increase efficiency. Exergetic analysis shows that energy resources have different qualities, while energy-saving methods, which are based on the first law of thermodynamics, consider all energy resources as equivalent. The load factor is an indicator of energy efficiency, which is determined by dividing the total energy consumed during the billing period by the maximum possible energy consumption for this period. This coefficient can be used to determine the potential reduction in exergy consumption by postponing operations, replacing or eliminating oversized equipment, and replacing

continuously operating equipment with more efficient alternatives. In addition, an idea is given of how thermodynamic principles, the first and second laws of thermodynamics, can be applied to calculate mass flows and transfer of energy, work, and heat across the boundary at the state temperature. The main argument of this study is that the change in entropy between two states for ideal gases, as indicated in the ideal gas law, depends on both temperature and pressure. In addition, the study provides a comprehensive overview of the content of thermochemical exergy in the flow under various environmental conditions, including the absolute enthalpy of formation and entropy considerations. This emphasizes the practicality and accuracy of calculating the optimal shift scheme based on the load factor and the possibility of reducing energy costs when using the billing model during use. The use of a load factor is considered to identify electricity billing errors, allowing energy managers to identify and correct errors. It is also a practical tool for evaluating the efficiency, effectiveness, and potential of an energy-intensive process. As a result, it can be concluded that exergetic analysis is an effective and efficient tool for optimizing and improving industrial processes, which leads to lower costs and increased productivity [24].

This study describes the latest developments in the use of control and optimization to improve energy efficiency and reduce the irreversibility of energy in networks. It is revealed that operations based on exergy lead to significantly higher energy efficiency compared to traditional methods and can reduce irreversibility. Exergetic analysis makes it possible to identify thermodynamic defects. Work and heat can be controlled and optimized separately. Throughout the United States, 2.5 gigatons of energy is consumed annually, of which only 11% is from renewable energy sources. Current and future integrated energy systems are expected to benefit from exergy analysis by improving energy efficiency. The study presents the possibilities and advantages of merging exergy analysis with process management and optimization solutions for integrated energy systems. Several works have been consulted over the past decade to explore the potential of energy-based operations in both the industrial and residential sectors. The works of Gibbs, Rant, Szargut, Brodysansky, and Kotas demonstrate the use of exergy to optimize efficiency in industrial processes and thermal installations. The study demonstrates the possibility of using linear quadratic regulator (LCR) approaches for boilers and Hamiltonian algorithms for optimal control of electrical microgrids to reduce the destruction of exergy. Exergy optimization has been applied to systems such as solar collectors, regenerative Brayton cycles, trigeneration plants, gas turbines, and internal combustion engines (ICE). On average, it has been found that the use of load optimization increases efficiency, reduces carbon emissions, and achieves fuel savings of up to 6–7%. The Predictive Control Model (MPC) was used to optimize heating, ventilation, and air conditioning systems of buildings, reducing energy consumption and destruction. It was also used to reduce friction and final temperature differences in the fluid flow and optimize multi-input, multi-output processes. There is potential for optimization and exergy control to improve existing processes and further reduce energy consumption and carbon emissions. This research requires further advances in the integration of complex energy systems in order to lead to a more efficient use of energy and promote more environmentally friendly and sustainable energy in the future [25].

The study examines the use of two types of combined CO<sub>2</sub>-based cycles powered by an LM2500+ gas turbine for electricity generation. It was found that the efficiency of CO<sub>2</sub>-TC + OTC is higher than that of CO<sub>2</sub>-TC/OTC. Carbon dioxide (CO<sub>2</sub>) is attractive for waste heat recovery in medium and high temperature sources due to its high thermal stability and ideal heat and mass transfer properties. By optimizing the parameters using a genetic algorithm, the net output power of the combined cycle can be maximized. The Organic Transarctic Cycle (OTC) uses lower critical temperatures and dry isentropic characteristics of organic working fluids. The solution is to introduce a recuperator to recover heat from the exhaust gases of the turbine and increase the thermal efficiency of the cycle. Echogen Power Systems LLC has linked this recuperative supercritical cycle (SC) with a waste heat recovery system. The influence of other cycle parameters on system performance is also

considered. Parametric optimization was performed using Matlab and Genetic Algorithm; the results indicate better thermodynamic performance for two combined cycles. Pentane is found to be superior to R134a, as it can extract more heat from the emitted CO<sub>2</sub> with lower thermal cycle efficiency. Energy losses in each component are also analyzed. In CO<sub>2</sub>-TC/OTC, the greatest energy losses occur in a steam generator with heat recovery, followed by an intermediate heat exchanger, which is explained by poor temperature compliance. The main conclusion is that the net output power and thermal efficiency of the combined cycle increase with increasing CO<sub>2</sub> heat addition pressure [26].

This study provides an energy, exergetic, and economic comparison of three solar-powered trigeneration systems suitable for buildings with high energy needs. The systems consist of an organic Rankine cycle, a parabolic solar collector, and various heat pumps. The results show that System 1 has the best energy, exergetic, and economic indicators of the three systems. It has the highest energy efficiency (78.17%), exergetic efficiency (15.94%), and the shortest simple payback period (5.62 years). It also produces 6.05 kW of electricity, 25.28 kW of heat, and 23.39 kW of cold. System 2 has an intermediate performance with an energy efficiency of 43.30%, an exergetic efficiency of 13.08% and a simple payback period of 7.82 years. System 3 is the least efficient with an energy efficiency of 37.45%, an exergetic efficiency of 8.49%, and a simple payback period of 8.49 years. The combination of the organic Rankine cycle with absorption chillers turns out to be an effective solution for the production of heat and cold. This type of trigeneration system can be used to meet high energy needs in commercial buildings and hospitals, as well as in apartment buildings. The systems under study were modeled using thermodynamic and dynamic models in the Engineering Equation Solver and FORTRAN programs. The results were based on the location of the study; in this case, the research was conducted in Athens, Greece. Sensitivity and optimization analyses provide a better understanding of system performance and allows for the optimization of a simple payback period. This research is a step towards the development of efficient and cost-effective trigeneration systems. This gives an idea of the key parameters that should be taken into account when developing and evaluating various trigeneration systems. The findings of this study can be used as a reference material in the design and optimization of trigeneration systems powered by solar energy worldwide [27].

In this article, a one-dimensional model of a Tesla turbine was built to make it equally applicable to the conditions of a two-phase flow of wet working fluids. The model of the Tesla turbine and ORC system was constructed from a thermodynamic point of view, and five typical wet working fluids (R22, R417a, R134a, R152a, and R290) were selected to study the effect of five wet working fluids on the thermal characteristics of the Tesla turbine and ORC system. The effect of changes in the key design parameters of the Tesla turbine on the performance of the Tesla turbine and the ORC system was further analyzed when using various wet working fluids in the ORC system. The results showed that the highest turbine efficiency of 42% was achieved when the Tesla turbine used R22 as the working fluid under design conditions, while the highest turbine power output and the highest thermal efficiency of the system of 1.19 kW and 3.96% were achieved when R417a was used as the working fluid. The analysis of the key structural parameters of the system showed that for five different wet working fluids, the efficiency of the turbine, the output power of the turbine, and the thermal efficiency of the system monotonically increased with an increase in the input radius of the rotor. For each of the five wet working fluids, there is an optimal rotor speed, the radius of the rotor outlet and the distance between the rotors, which ensures optimal turbine efficiency and system performance. The corresponding work is an important guideline for the optimal design of Tesla turbines with wet working fluids [28].

This review study focuses on the use of the Rankine solar organic cycle and its applications for polygeneration. This article discusses new experimental and numerical studies by various researchers devoted to the Rankine solar organic cycle with different integration of solar collectors together with various organic working fluids. The review study mainly focuses on the applications of cogeneration, trigeneration, and polygeneration of

the Rankine solar organic cycle. In the end, the future part of this study will undoubtedly help researchers and engineers in further improving the Rankine solar organic system [29].

In this study, the advantages of ORC were used to improve the overall performance of a simple gas turbine (GT) located in a wood production facility. In addition to the ORC, the steam boiler (SB) is also connected to the GT to increase overall productivity and produce the necessary steam. During the research, benzene, cyclohexane, hexane, P11, P123, P600, P601, and toluene were used as the working fluid. With parametric optimization of the ORC, the pressure at the turbine inlet increased from 10 bar to 35 bar, and the pressure at the turbine inlet increased from the saturated steam temperature to the maximum liquid temperature. The best working fluid was benzene for the pressure at the inlet to the ORC turbine from 10 to 25 bar. With an ORC turbine inlet pressure above 25 bar, the R123 showed the best performance. The maximum useful power of ORC, thermal, and exergetic efficiency were 1076.76 kW, 21.14%, and 47.00% for ORC using R123 at 230 °C and 35 bar. However, although the ORC with R123 has the highest useful power generation, the payback period of the ORC with R11 is minimal (2.5 years). With these input parameters of the ORC turbine, the operating parameters of the cogeneration system turned out to be the highest: thermal efficiency 69.19% and exergetic efficiency 75.51% [30].

In this study, simple and regenerative organic Rankine cycles (ORCS) were developed as the lower cycle of a simple gas turbine. After the design, the performance of the ORC engines was analyzed when the temperature and pressure at the turbine inlet changed. The study selected eight different working fluids for ORC design to determine the most effective working candidate, namely benzene, cyclohexane, ethanol, methanol, R21, R152a, toluene, and trans-2-butane. At all values of the pressure at the turbine inlet, the maximum characteristics were obtained by using methanol for simple ORC (sORC) and trans-2-butane for regenerative ORC (rORC). The maximum useful power, thermal efficiency, and exergetic efficiencies of sORC were obtained with methanol at 45 bar and 350 °C, reaching 1967 kW, 24.5% and 48.9%, respectively. For the RRC, the maximum useful power, thermal efficiency and exergetic efficiency were obtained with trans-2-butane at 40 bar, 240 °C and amounted to 2523 kW, 31.1% and 62.4%, respectively. The highest useful power, thermal efficiency and exergetic efficiency of the combined cycle of a gas turbine (GT)-ORC are detected at 40 bar and 240 °C for rORC, reaching 8723 kW, 47.63%, and 67.33%, respectively. This means that almost 1605 kg—CO<sub>2</sub>/h 1.605 kg-CO<sub>2</sub>/h of reduction in CO<sub>2</sub>CO<sub>2</sub> emissions is possible when using rORC as the lower cycle in GT. When considering the total heat input from the fuel in the GT burner, it can be seen that the generation of electricity in the combined GT-rORC cycle can be increased up to 40.7%. In order to determine optimal performance in real operating conditions, the developed system can be used by ORC engine developers, manufacturers, and at facilities where simple gas turbines are available [31].

In this paper, a thermodynamic and parametric analysis of the proposed system is proposed, in which various mixtures of zeotropic liquids are used as a working fluid in the ORC and ERC cycles. The integration of ORC and ERC systems with zeotropic mixtures provides a significant opportunity to combine their superiority and significantly improve system performance. The superiority of the proposed system, which combines the advantages of zeotropic mixtures with the positive sides of ORC and ERS, is revealed using energy and exergetic analysis. The results revealed some valuable facts. For example, the total thermal and exergetic efficiency are calculated using the formula 18.16% and 59.16%, respectively. In addition, the COP and cooling capacity of the ERC unit are 0.1224 and 93.73 kW, respectively. In addition, the best exergetic efficiency and the least exergetic destruction are estimated for a system with isopentane (0.3)/R142b (0.7) as the working fluid. In addition, from the parametric study, it can be concluded that a decrease in pressure in the separator and an increase in temperature at the inlet to the heat exchanger leads to higher energy and exergetic efficiency [32].

### *2.5. Methods of Optimization of Designs of Heat Pumps and Equipment of the Organic Rankine Cycle*

Urban untreated wastewater is widely used as a heat source in the heat pump system. Wastewater energy is usually extracted indirectly, i.e., by installing a heat exchanger in front of installations. A shell-and-tube heat exchanger is widely used among sewer heat exchangers, while a heat pump system with a source of untreated wastewater using a plate heat exchanger is less common due to its special design requiring a higher quality of wastewater treatment and a better treatment method. To solve this problem, a specially designed heat pump system with a wastewater source was developed and tested. It consists of a kind of pre-treatment device, i.e., a spiral filter for wastewater of its own design and a plate heat exchanger for wastewater with automatic backwash. The model of the heat transfer coefficient of a plate heat exchanger is verified by comparing the actual operating data with the theoretical value, and then the effect of the wastewater flow rate on the heat exchanger is analyzed. Finally, the COP value is calculated and the energy saving efficiency of the entire system is evaluated. The filtering device has a good clogging prevention effect, and the heat exchanger operates stably, achieving the expected energy-saving effect. In addition, the energy-saving efficiency of the entire system is evaluated. The test results in real operation show that the COP value of the new wastewater-based heat pump system proposed in this article is 3.02 [33].

Many international protocols insist on replacing harmful substances that accelerate global warming. As a solution, it is recommended to use the Rankine cycle, a means of recovering waste heat from small and low-grade heat sources in various applications, such as industrial waste heat, biomass solar energy, geothermal energy, and turbine exhaust gases. This is an efficient technology for generating electricity from waste heat or free energy sources. The authors conduct a study aimed at choosing the safest in many senses, and the most effective working body of the cycle [34].

Microturbines (<100 kW) are commercially used as expansion machines in waste heat recovery (WHR) systems such as Organic Rankine Cycles (ORCs). These high-loaded turbines, as a rule, are designed for a certain set of parameters, and their isentropic expansion efficiency deteriorates significantly when the mass flow rate of the WHR system deviates from the calculated value. However, in many industrial processes that are potentially interesting for the implementation of the WHR process, the temperature, mass flow rate, or both can fluctuate significantly, which leads to fluctuations in the WHR system as well. In such circumstances, the pressure at the inlet of the ORC turbine and, consequently, the efficiency of the reversible cycle should be significantly reduced during these failures. In this context, the authors have developed an adaptive supersonic microturbine for use in the WHR mode. The variable geometry of the turbine nozzles allows you to adjust the throughput depending on the available mass flow rate to maintain a constant pressure of the upper cycle. This article analyzes a series of experimental tests of the WHR ORC test stand equipped with the developed adaptive supersonic microturbine. An adaptive turbine is characterized with respect to its non-design characteristics, and the results are compared with a reference turbine with a fixed geometry. In order to create a reliable database for this comparison, a digital duplicate of the installation was created based on experimental data. In addition to the characteristics of the turbine itself, the effect of the improved pressure ratio on the energy conversion chain of the entire ORC is analyzed [35].

Based on the experiment, the authors conducted an energy and exergetic analysis of a plate heat exchanger using a hybrid nanofluid as a refrigerant to study the effect of the volume ratio of nanoparticles at different nanofluid flow rates and inlet temperatures. Correlations are proposed for predicting the Nusselt number for both DI-water and hybrid nanofluid. The study shows that the energy and exergetic characteristics continuously decrease with an increase in the TiO<sub>2</sub> content in the mixture, which does not lead to an optimal ratio of nanoparticles in the mixture [36].

This article is devoted to the study of a clothes dryer with a heat pump connected to a heat exchanger. The aim is to study the effect of a heat exchanger on the performance of a heat pump dryer.

The results show that the presence of a heat exchanger increases the performance of a heat pump dryer. This is due to the fact that the heat exchanger provides better drying conditions in a drying room with a higher temperature and lower relative humidity compared to a dryer with a heat pump without a heat exchanger. The efficiency of the heat exchanger is also high, as it exceeds 50%. It is recommended to install a heat exchanger in a dryer with a heat pump [37].

This study examined the optimal design of a capillary heat exchanger for a heat pump system and its application in a building. The overall goal was to use a capillary heat exchanger to generate energy in coastal areas to promote renewable energy sources in the design of low-carbon buildings. Initially, the main factors affecting the efficiency of the capillary heat exchanger were determined. Then, a mathematical model was created to analyze the heat transfer process. The analysis showed that the flow rate and capillary length are key factors affecting the efficiency of the capillary heat exchanger. Secondly, to optimize the design of the capillary heat exchanger, the transfer of thermal energy is calculated for different capillary lengths at different flow rates in summer and winter conditions, respectively. Thirdly, a typical building was chosen to analyze the use of a capillary heat exchanger for energy extraction in the coastal zone. The results show the performance of the selected heat pump system with a capillary heat exchanger. In winter, the heat transfer rate is  $60 \text{ W/m}^2$  at a seawater temperature of  $3.7 \text{ }^\circ\text{C}$ . In summer, the heat transfer rate is  $150 \text{ W/m}^2$  at a seawater temperature of  $24.6 \text{ }^\circ\text{C}$  [38].

For the plate heat exchanger of the heat pump system, the ratio of the convection heat transfer of the condenser and the evaporator was used to simulate the heat transfer of the heat exchanger. In addition, an experimental test of the heat exchanger was carried out in the heat pump system. The results of numerical simulation were compared with experimental results. The results show that the average error between the results of numerical simulation of the condenser and evaporator and the experimental results is 5.75% and 1.13%, respectively, which proves that the simplified hypothesis, the heat transfer model, and the solution method used in numerical simulation are reasonable for the evaporation and condensation process of a plate heat exchanger for a heat pump [39].

The authors describe a brazed-type plate heat exchanger consists of a series of wave overlays of sheet metal forming a new type of highly efficient heat exchanger. Heat exchange with a passage through the sheet between them, in comparison with a traditional heat exchanger, has a compact design, low cost, high-heat transfer coefficient, low pollution coefficient, and a number of advantages. Thanks to the field of cooling and air conditioning, it has a very wide prospect of application in the market. Due to the complexity of the mechanism of phase transition and two-phase heat exchange, a strict theoretical conclusion is difficult [40].

This paper presents a mathematical model of heat pump heat exchangers and their thermal interaction with a fan for an air dryer. The calculation algorithm developed for finned heat exchangers is based on the  $\varepsilon$ -NTU method, which allows for the determination of the heat transfer coefficients from the air and refrigerant, the heat capacity of the evaporator and condenser, and the parameters of the air at the outlet of the dryer with a known geometry of the heat exchanger, initial air parameters, and mass flow. The model was tested on the test bench of an industrial dehumidifier. This made it possible to calculate the heat transfer coefficients for the heat exchanger depending on the speed of rotation and, consequently, the power of the fan drive motor. An increase in fan performance, on the one hand, leads to an increase in the heat transfer rate. However, on the other hand, it leads to an increase in the overall energy consumption of the engine. Thus, although this leads to an increase in drying performance, it also leads to an increase in the energy consumption of the dehumidifier. Therefore, in order to optimize the installation in terms

of energy consumption, it is necessary to define a function that relates to the amount and efficiency of heat emitted from the fan [41].

The purpose of this study was to develop a mathematical model with concentrated parameters for studying the energy parameters of a heat pump with an internal heat exchanger (IHX). The developed mathematical model has been confirmed by 25 tests using R134a as a working fluid. The results show that the maximum prediction error between the simulated and experimental results for CS is 7.06%. The main purpose of this work was to study the efficiency of the heat pump, as well as the efficiency of the internal heat exchanger, and present a new equation for calculating the COP value. When the IHX efficiency was increased from 0.65 to 0.95, the COP value increased by 5.41% at a minimum evaporation temperature of  $-20\text{ }^{\circ}\text{C}$  and a maximum condensation temperature of  $90\text{ }^{\circ}\text{C}$  [42–48].

### 2.6. Complex Using of Renewable Sources: Prerequisites for Creating a Methodology Combining Elements of Thermodynamic Analysis and Exergetic Calculation Method

Thermodynamic and exergetic methods are used to analyze the performance of installations, processes, and calculation methods from the point of view of energy efficiency and system stability [49]. Thermodynamic analysis is used to calculate the heat losses, the supplied, and generated energy of the system, and the exergetics method is used to calculate the potential for improving the stability of the system. Thermodynamic and exergetic methods can be used together to determine the potential for improving both energy efficiency and system stability. Where the authors of the projects consider each of the methods in detail.

Exergetic analysis is an invaluable tool for evaluating the efficiency of energy systems. It allows for an estimation regarding the amount of energy consumed or produced, as well as the quality of energy resources used in energy-consuming and energy-producing installations. Combining quantitative and qualitative measurements, exergetic analysis can identify the most inefficient components of energy-related technologies and suggest ways to reduce energy losses. This improved understanding of energy systems allows engineers to design more efficient systems and maximize their performance.

The authors of the project conducted research on potential solutions to maximize the efficiency cycle of a thermal power plant by studying the potential of including renewable energy sources in the existing cycle. Figures 1 and 2 show the main schemes of the research carried out at the early stages.

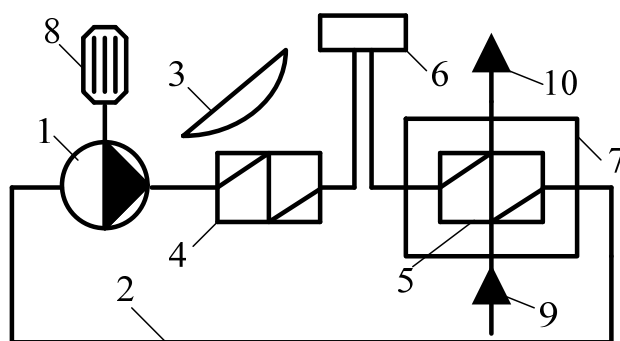


**Figure 1.** Scheme of air cooling and water heating of an electric generator: 1—Pump; 2—Water supply; 3—Solar concentrator; 4—Heat pump; 5—Water–air heat exchanger; 6—Heated water flow; 7—Electric generator; 8—Electric drive; 9—Atmospheric air inlet; 10—Atmospheric air outlet.

In addition, the authors of [50] of the work investigated the potential of using the cooling system shown in Figure 3, and whether it can be improved by including an organic Rankine cycle.

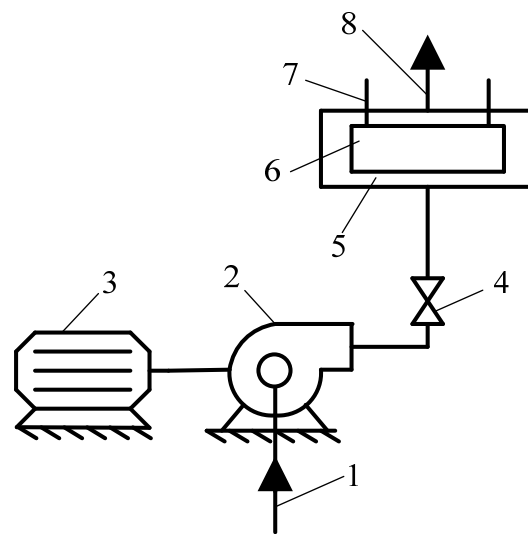


**Figure 2.** The old scheme of air cooling of the electric generator: 1—Atmospheric air input; 2—Centrifugal fan; 3—Electric drive; 4—Shut-off valve; 5—Electric generator; 6—Water–air heat exchanger; 7—Water; 8—Atmospheric air output.

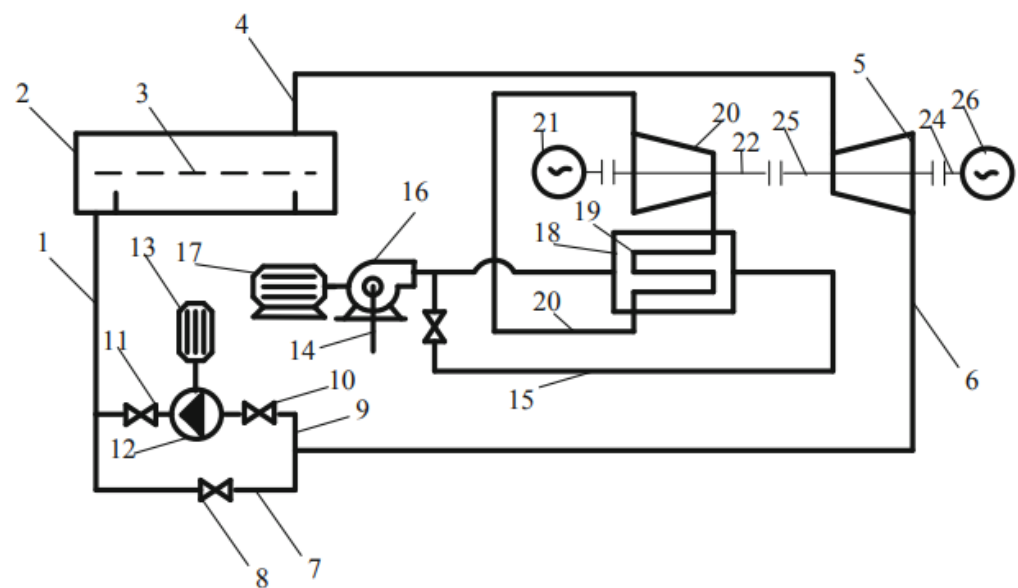


**Figure 3.** This scheme offers the use of renewable energy sources for combined generation of cold and electricity (Notation further in the text).

In the panel system of Pipes 1, a low-boiling coolant circulates, operating on the principle of a solar collector. The panels of the Pipeline System 1 are installed along the vertical walls of the production room. In the daytime, the coolant rises because of the difference in densities, as well as the forces of natural convection arising due to heating by electromagnetic (thermal) radiation from the sun. When the Drum 2 is installed on the roof of the building, it separates the coolant droplets from the steam in the Separator 3. Dry saturated Steam 4 is formed, which is fed into the Turbo Expander 5. The shaft of the Turbo Expander 25 is connected to the electric shaft of the Generator 26, which generates electricity for the company's own needs. After the Turbo Expander 5, the steam condenses and returns to the cycle through the Pipeline 6 in the form of condensate. During the daytime, the condensate is routed through the Open Valve 8 and the Pipeline 7. At night, the Pump 12 with an Electric Drive 13 is turned on with Fans 10 and 11 open. During the transition time, Pump 13 does not operate in the nominal mode due to the use of a

frequency-controlled Electric Drive 13. The industrial air conditioning circuit consists of two circuits: a cooling Air Circuit 15 and a heated Refrigerant Circuit 20. The air from Atmosphere 14 is pumped out by Fan 16 with an Electric Drive 17 and connected to a Heat Exchanger 18. The Heat Exchanger 18 consists of Tubes 19 in which freon is heated. Freon vapors are compressed in a Compressor 20 with Electric Drive 21. The Compressor Shaft 22 is connected to the Shaft 25 of the Turbo Expander 5.

In the study [44], the authors considered the work of the organic Rankine cycle. In addition to traditional energy sources, there are other types of renewable resources, such as photovoltaic panels and solar collectors.

The superheated steam-water medium from the power boiler of the power unit is sent to the downpipe, passing along the way through the economizer and the air heater. Feed water is heated when passing through the economizer and entering the heat treatment system before getting into the overheating process, with air moving from the boiler drum to the air heater through a fan. The air heater in the system is powered by fuel—combustion or preparation, depending on the type of fuel used and the power of the fuel gas supply device. Exhaust gases are cooled to a temperature of 120 °C before entering a convective heat exchanger with a dynamic nozzle [50]. This nozzle directs the cooled water through the piping system, while fuel gas particles mix with the water as it passes through the nozzle. Some of the triatomic gases, including CO<sub>2</sub> and NO<sub>x</sub>, are aerated with water and pass through the heat exchanger to the lower part of the chimney.

The gas-enriched water supplied by the pipeline system is fed into an improved absorption Li–Br refrigeration unit. The uniqueness of this refrigerating machine lies in the presence of a solar radiation heating unit. The heating elements are installed in gas-enriched water in a separate unit, allowing the refrigerator to be used even at low temperatures. An element is installed in the water heating chamber. It can have a convex or concave parabolic shape. Compartments and dividing partitions are located in the chamber. Water is supplied to the heating unit, where it is heated and cycled. Then, it enters the Chemical Treatment Unit and the heat exchangers of the chemical water treatment unit pass water into the main deaerator and heat exchangers. Then, the entire water flow is sent to the boiler unit economizer, and the cooled return water is a deaerator, which contains a deaeration column and a tank with a monoethanolamine solution. The steam coming out of the deaerator is sent to a storage facility filled with a calcium chloride solution capable of removing any nitrogen and sulfur oxide particles. Then, the gases are extracted from the tank and sent to the separator. After passing through the heat exchangers of the raw water treatment plant, the purified water circulates and cools in the evaporator of the absorption refrigerator. Then, the mixture of raw water and water passed through the heat exchangers is pushed by a heat pump and fed into the absorber of the absorption refrigerator. The resulting feed water exits the system. The remaining materials are processed.

Thus, in the study [44], the authors touched upon the topic of greenhouse gas capture. In [45], the authors evaluated the potential of using a heat pump and an organic Rankine cycle for the use of renewable energy sources in desalination systems. Comparing the Rankine, Stirling, Brayton, and Kalina cycles, it was noticed that the Rankine cycle has greater versatility and adapts to various sources of thermal energy. The main calculated dependences were compiled using standard energy balance methods. Figure 4 shows one of the possible configurations of the circuit. Figure 4 shows one of the variants of the scheme.

To place a heater in a desalination system in combination with a heat pump, it is necessary to apply a new approach to evaluate the effectiveness of the system. Instead of relying solely on thermodynamic energy balances, the exergy method should be included in the methodology.

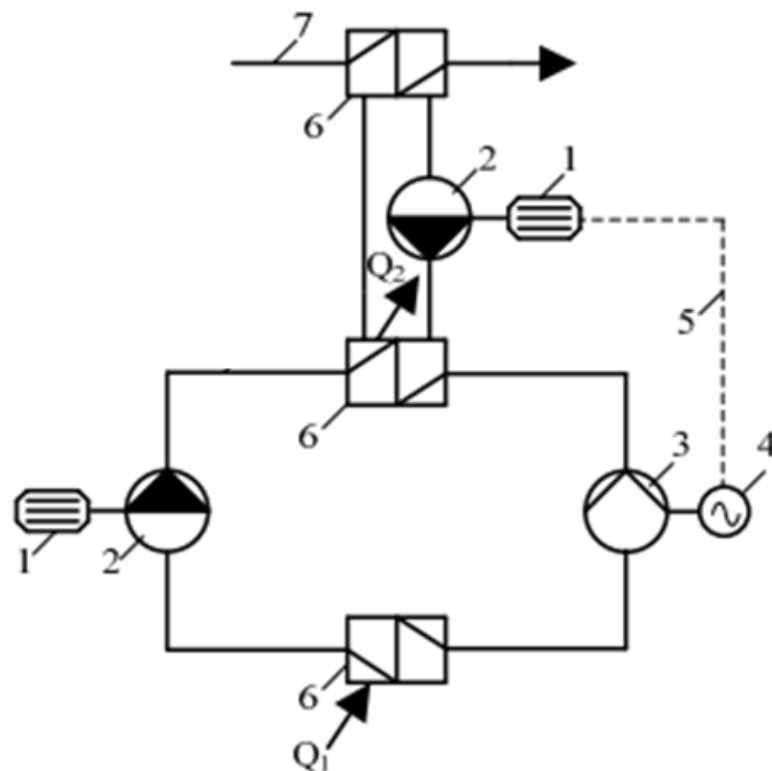


**Figure 4.** Technological scheme using organic Rankine cycle: 1—Electric drive; 2—Pump; 3—Expander; 4—Electric generator; 5—Electric cable; 6—Heat exchanger; 7—Water heating line.

### 2.7. Energy Analysis Applied to Organic Rankine Cycle Systems

Energy analysis applied to Organic Rankine Cycle (ORC) systems is a valuable tool for evaluating the performance and effectiveness of these systems. This includes the analysis of energy flows and transformations within the ORC system to determine the overall distribution of energy across components. This analysis helps to identify areas where thermal efficiency can be improved by optimizing operating parameters, such as evaporation pressure or condensation temperature.

Here is a step-by-step explanation of how energy analysis is applied to ORC systems and its benefits:

- **System Boundary:** The first step is to define the boundary of the system, which includes all the components involved in the ORC system. As a rule, the ORC system consists of a heat source, an evaporator, an expander (turbine), a condenser, a pump, and a working fluid.
- **Energy flows:** Next, energy flows within the system are identified and quantified. This includes the heat supply from the heat source to the evaporator, the output power of the expander, and the heat removal from the condenser to the cooling medium. The pump operation required for the circulation of the working fluid is also taken into account.
- **Energy balance:** The energy balance equation is applied to the ORC system taking into account the energy flows in each component. This balance equation ensures that the energy entering the system is equal to the output energy, and any loss or gain of energy is taken into account.
- **Efficiency analysis:** After quantifying the energy flows and establishing the energy balance, various efficiency parameters can be calculated. These include thermal efficiency, which is the ratio of total output to heat consumed, as well as the efficiency of components such as evaporator efficiency, turbine efficiency, and pump efficiency.

Advantages of energy analysis in ORC systems:

- **Total Energy Consumption:** Energy Analysis provides a comprehensive breakdown of total energy flows in the ORC system. This helps to understand the distribution of energy between different components and processes, allowing for a detailed assessment of system performance.
- **Inefficiency Detection:** Energy analysis helps to identify areas where energy loss or inefficiency occurs in the ORC system. By quantifying the energy flows in each component, it becomes possible to pinpoint specific locations or processes where improvements can be made to improve overall efficiency.
- **Optimization of operating parameters:** Energy analysis allows you to evaluate various operating parameters, such as evaporation pressure or condensation temperature, and their impact on system performance. By analyzing the energy flows under various scenarios, it is possible to determine the optimal operating conditions, which will lead to an increase in thermal efficiency.
- **Design and Retrofitting:** Energy analysis is valuable at the design stage of an ORC system, as it helps in selecting suitable components, determining their technical characteristics, and evaluating expected performance. It is also useful for upgrading existing ORC systems, as it allows you to identify potential areas for improvement and optimization.

Thus, energy analysis applied to ORC systems provides a comprehensive understanding of energy flows and system efficiency. This allows for the distribution of the total energy among the components, identification of shortcomings, and optimization of the operating parameters to increase thermal efficiency. This analysis is useful both for designing new ORC systems and for optimizing existing ones.

### 3. Discussion and Future Prospects

#### 3.1. Methodology: A Case Study of Energy Technological Complex

The methodology considered by the authors is a scientific approach to solving the problems of calculating efficiency and optimization in the design of energy technology complexes combining a heat pump (including a turbo expander for the implementation of the organic Rankine cycle), a photovoltaic panel, a desalination plant, an optional solar concentrator (solar concentrator), and a wind generator. In addition, the scientific approach does not deny the possibility of working not only on the Rankine cycle, but also on the Kalina cycle, since the methodological base does not change.

Figure 5 shows the basic scheme of the energy technology complex, which can be implemented at the expense of the grant.

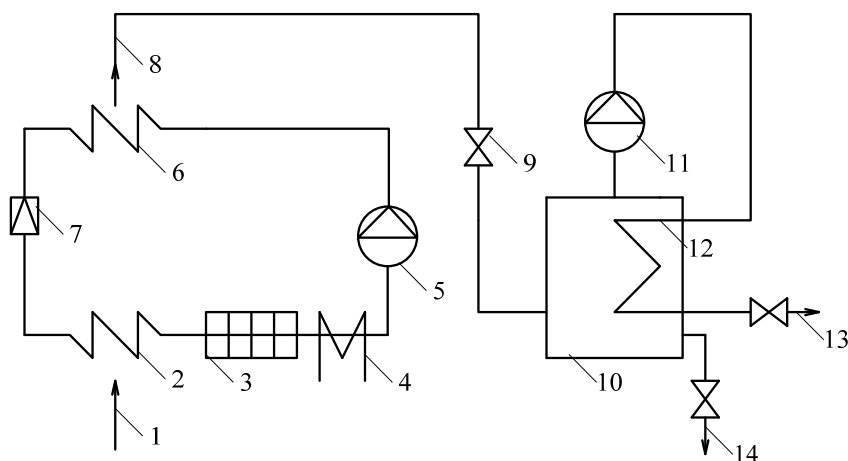


Figure 5. Basic scheme of the energy technology complex.

Figure 5 shows the basic technological scheme underlying the methodology. The designations are as follows: 1—Low-temperature heat source; 2—Evaporator; 3—Photovoltaic panel; 4—Additional (backup) heater; 5—Compressor; 6—Condenser; 7—Expander (capillary tube); 8—Heated water; 9—Valve; 10—Main desalination tank; 11—Steam compressor; 12—Distillate condenser heat exchanger; 13—Desalinated water outlet; 14—Salt water outlet.

Figure 6 demonstrates an improved technological scheme. Elements with which the scheme is supplemented: 15—Turbo expander; 16—Wind turbine; 17—Solar concentrator (solar concentrator).

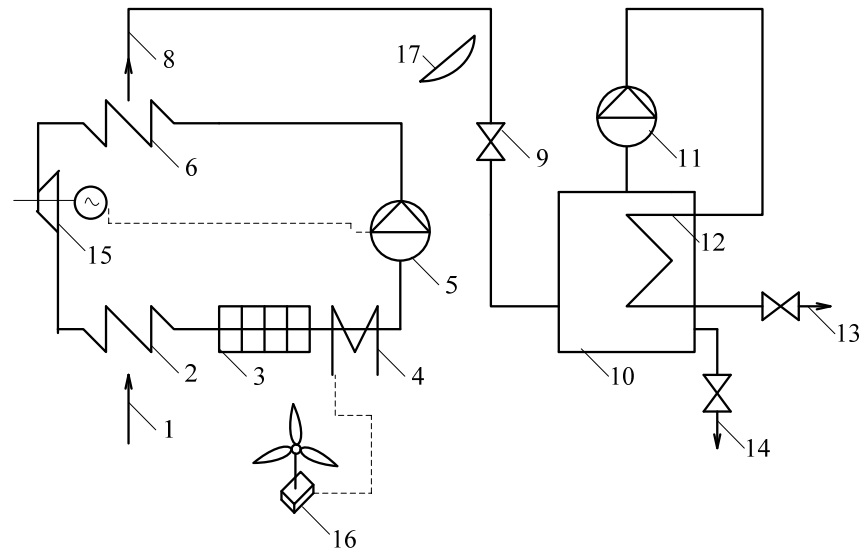


Figure 6. Improved technological scheme of the desalination plant.

The scheme according to Figure 7 can also work according to the Kalina cycle. There are no fundamental differences.

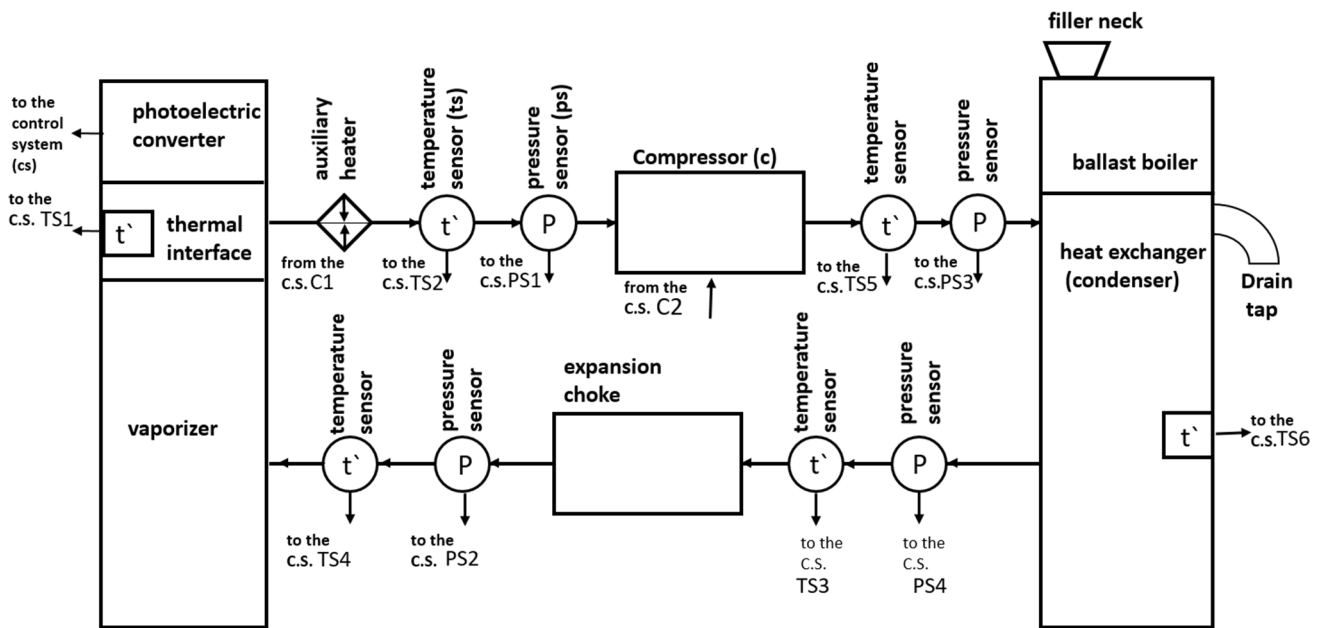


Figure 7. Schematic diagram of the installation.

Combining the methods of energy balances of thermodynamic analysis and the exergetic method when used in the main scheme is also useful.

The purpose of the methodology is to determine the thermal coefficient of the cycle  $\epsilon$ . The determination of the amount of Heat  $Q_2$  was required by the heater. The estimation of the amount of Heat  $Q_1$  was transferred to the water. The construction of the process in Diagram P-i was used for Refrigerant R407C.

By installing a heat pump, consumers can take advantage of many advantages of a more energy-efficient and environmentally friendly heating system. This technology allows heat to be transferred from colder sources to hotter areas, allowing energy to be extracted from sources that would otherwise be wasted, such as wastewater, sewage treatment plants, and air. This heat transfer gives users almost two times more heat than they receive with direct combustion. In addition to saving energy, this form of heating also reduces emissions and helps reduce the impact of climate change. Recently, heat pumps have become very popular and offer additional heating options other than traditional fuel means.

We study the operation of the cooling cycle according to the scheme shown in Figure 8. The working substance is freon R407c, which moves along the contour of the system. The evaporator works to convert a gaseous substance into a liquid at low temperatures and pressure. The compressor then compresses the liquid refrigerant, increasing the pressure to 12 bar and temperature to 85 °C. After passing through the compressor, the refrigerant enters the heat exchanger (condenser). Here, it emits its heat into the water, turning it back into a liquid form under pressure. Water is supplied to the system through the filler neck and exits through the drain tap. After the condensed refrigerant passes through the expansion valve, the pressure is significantly reduced, which leads to the evaporation of part of the liquid. This mixture of liquid and steam goes into the evaporator. The liquid turns into steam, evaporating under the action of the heat of the FEP or an additional heater. Due to this, boiling occurs in the evaporator, which consumes heat from the environment.

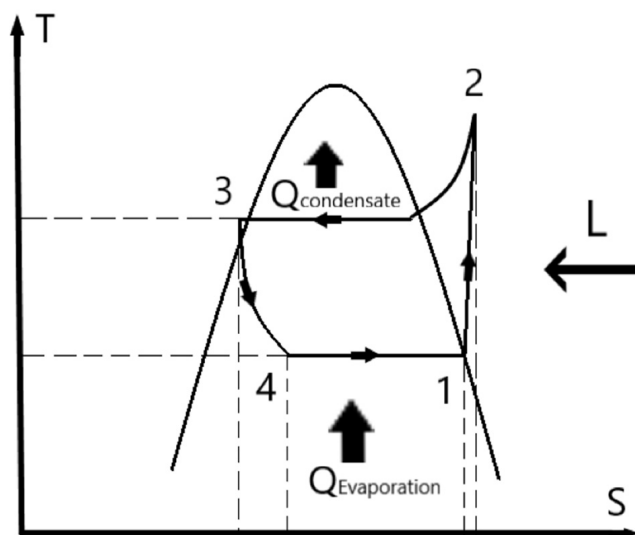


**Figure 8.** T-s diagram with heat pump cycle: 1–2—The process of adiabatic compression of the refrigerant in the compressor; 2–3—The process of heat removal from the condenser for water heating (pressure  $P_2$  and temperature  $t_2$  don't change); 3–4—Throttling process; 4–1—The process of heat supply to the evaporator (pressure  $P_1$  and temperature  $t_1$  don't change).

Then, the super-heated steam exits the evaporator, and the cycle repeats.

The unit is equipped with temperature sensors located behind the FEP and in the heat exchangers, as well as temperature and pressure sensors in front of and behind the compressor and expansion valve.

The heat pump cycle in the T–s–diagram is demonstrated in Figure 9. T—absolute temperature, K; s = dq/T—specific entropy is a thermodynamic parameter of the state, kJ/(kg·K).

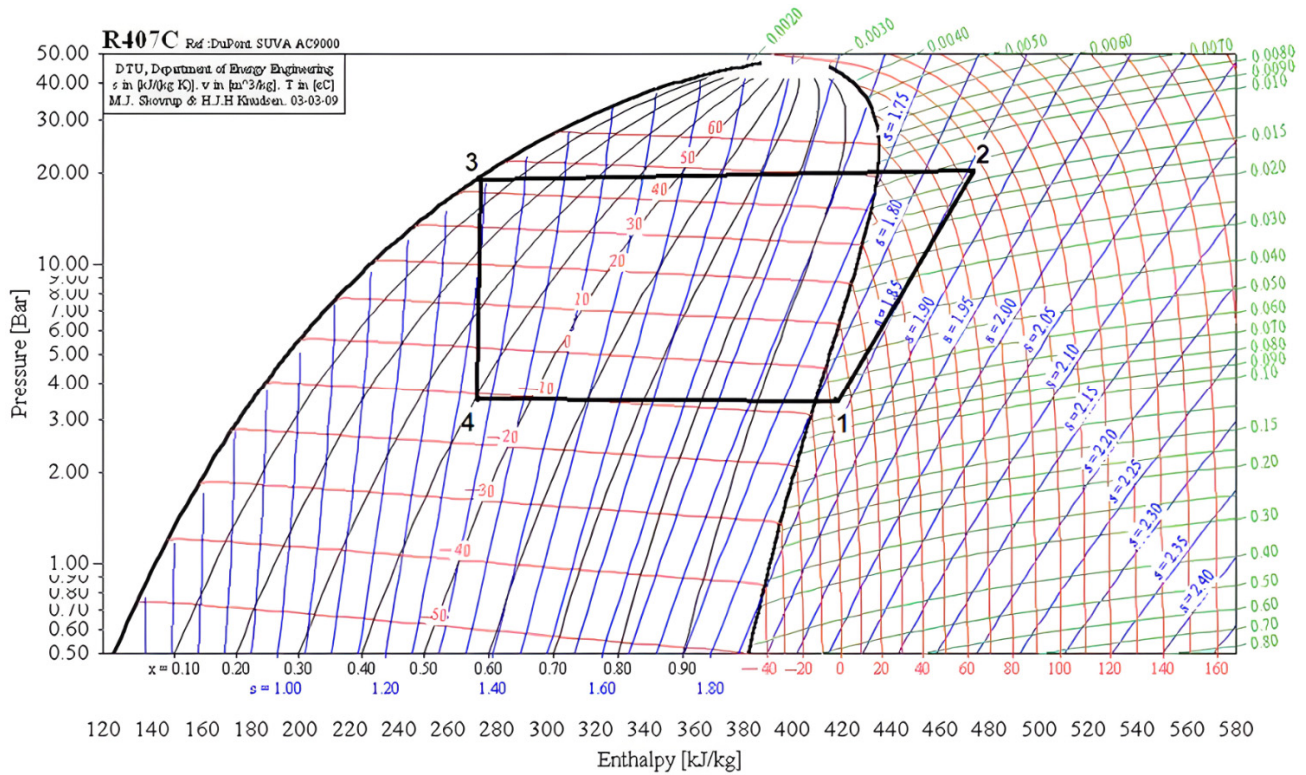


Figure 9. A heat pump cycle built on P–i diagram.

According to the known initial parameters of freon P1, T1, we observe a point on Diagram 1.

1. From the known data, we use the pressure and temperature from Sensor 3 and find Point 2 (after compression in the compressor). According to the data from Table 1 P4, t4 determines Point 4.

2. Draw a horizontal line from Point 2 to the saturation line and build a perpendicular line from Point 4. At the intersection of the straight lines, we insert Point 3.

Find Point 2a.

Knowing that the relation:

$$i_2 - i_1 = \frac{i_a - i_1}{\eta_a} \tag{1}$$

For freon compressors  $\eta_{ad}$ , with  $b = 0.0025$  is defined as:

$$\eta_a = \frac{T_0}{T_K} + b \cdot t_0 \tag{2}$$

Then, the enthalpy of Point 2a is determined by the formula:

$$i_a = \eta_a(i_2 - i_1) + i_1 \tag{3}$$

According to the received data, Table 1 is filled in.

**Table 1.** Experimental data.

Point Number	Pressure P		Temperature		Enthalpy $i$ , kJ/kg	Entropy $s$ , kJ/(kg·K)
	Bar	MPa	$t$ , °C	$T$ , K		
1	3.5	0.35	3	276	419	1.83
2	19	1.9	85	358	472.75	1.87
2	19	1.9	75	348	462	1.83
3	19	1.9	45	318	272	1.24
4	3.5	0.35	−11	262	272	1.275

The degree of dryness of saturated steam is expressed by the ratio of the mass of dry steam to the mass of wet steam. It can vary from 0 when the steam is in a liquid state to 1 when it is completely free of moisture [51]. This measurement can be used to determine the moisture content in saturated steam.

Find the degree of dryness at Point 1. Data on specific heat and cycle operation are also presented in Tables 2 and 3.

$$x_1 = \frac{s_1 - s_3}{s_2 - s_3} = \frac{1.83 - 1.24}{1.87 - 1.24} = 0.94 \quad (4)$$

**Table 2.** Specific heat and cycle operation.

Formula/Method of Determination	Value	Units of Measurement
$q_1 = h_2 - h_3$	200.75	kJ/kg
$q_2 = h_1 - h_4$	147	kJ/kg
$l_{\text{cycle}} = q_1 - q_2 = h_2 - h_1$	56.75	kJ/kg

**Table 3.** Characteristic mode of operation of the heating system.

Formula/Method of Determination	Value	Units of Measurement
$G = N/l_{\text{cycle}}$	0.003	kg/s
$Q_1 = q_1 \cdot G$	0.602	kW
$Q_2 = q_2 \cdot G$	0.441	kW
$\varepsilon = q_1/l_{\text{cycle}}$	3.5	-

When throttling, the production process is suspended and the energy consumption of the compressor corresponds to the power of the working cycle, which is 0.16 kW.

In order for the efficiency of the heating system to be justified, the heat produced must exceed the cost of the work required to create it. To do this, it is necessary to dispose of and use low-potential air heat that exceeds the cost of working in  $\varepsilon$  times [50].

### 3.2. Exergetic Method for Evaluating the Efficiency of a Heat Pump Installation

It is necessary to evaluate the efficiency of TNU. To achieve this goal, the following tasks are solved: determination of enthalpy, entropy, and exergy at characteristic points of the TNU cycle, construction of the TNU cycle in  $i$ - $s$  coordinates, as well as the compilation of the exergetic balance of TNU.

Based on the known parameters of the characteristic points of the cycle ( $P$ ,  $T$ ,  $i$ ,  $s$ ,  $e$ ), it is possible to construct this cycle in  $i$ - $s$  coordinates, which is shown in Table 4. Then, these indicators can be analyzed [50–52]. The TNU cycle graph is shown in Figure 10.

**Table 4.** Characteristics of the refrigerant at characteristic points.

Point Number	Pressure $P$		Temperature		Enthalpy $i$ , kJ/kg	Entropy $s$ , kJ/(kg·K)	Exergy $e$ , kJ/kg
	Bar	MPa	$t$ , °C	$T$ , K			
1	3.52	0.352	2.88	275.88	419	1.84	33.81
2	19	1.9	85	358	474	1.86	82.95
3	19	1.9	44	317	270	1.24	60.61
4	3.52	0.352	−11	262	270	1.275	50.355

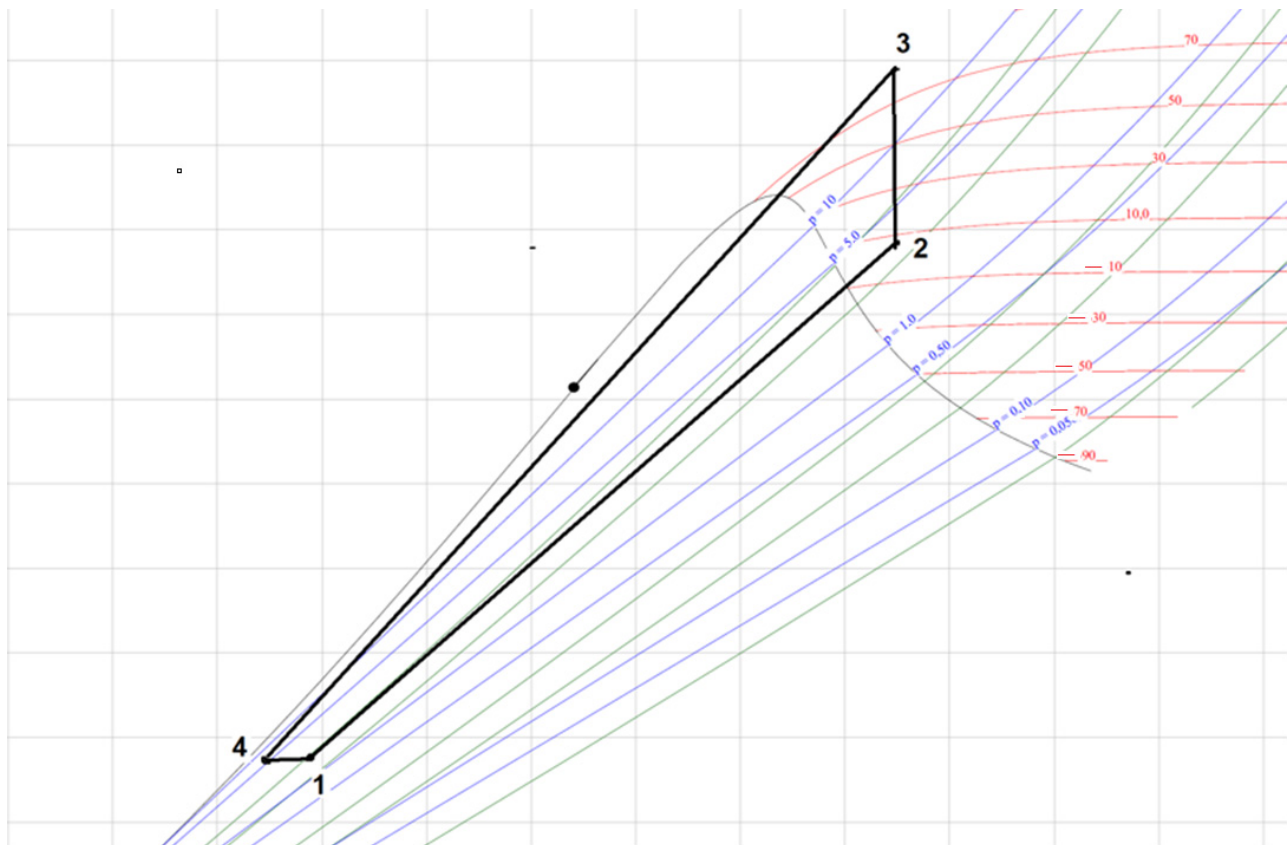
**Figure 10.** TNU cycle in  $i$ - $s$  coordinates.

Diagram LG  $p$ - $i$  is used to calculate enthalpy  $i_{n.e.}$  and entropy  $S_{n.e.}$ . The ambient temperature for this refrigerant at  $T_{n.e.}$  and pressure  $P_{n.e.} = 98.1$  kPa (1 atm). The intersecting isotherm and isobar determine the values of enthalpy and entropy of the refrigerant [53]. The following are Tables 5–7.

**Table 5.** Values of parameters for calculating specific exergies of refrigerant at characteristic points.

Parameters	Meaning	Units of Measurement
$I_{n.e.}$	435	kJ/kg
$S_{n.e.}$	2.01	kJ/(kg·K)
$T_{n.e.}$	293	K

**Table 6.** Values of specific exergies of the refrigerant at characteristic points.

Point	Meaning	Units of Measurement
	$e = i - T_{n,e} \cdot s - (i_{n,e} \cdot S_{n,e})$	
$e_1$	33.81	kJ/kg
$e_2$	82.95	kJ/kg
$e_3$	60.61	kJ/kg
$e_4$	50.355	kJ/kg
	$\Delta e = e_{i+1} - e_i$	
$\Delta e_{2-1}$	49.14	kJ/kg
$\Delta e_{3-2}$	22.34	kJ/kg
$\Delta e_{4-3}$	10.255	kJ/kg
$\Delta e_{1-4}$	16.545	kJ/kg
	$\Delta e_{dse} = \sum \Delta e$	
$\Delta e_{dse}$	0	kJ/kg

**Table 7.** Characteristic values of the cycle.

Formula/Method of Determination	Value	Units of Measurement
$V_o = G_s \cdot v_1$	0.00024	m <sup>3</sup> /s
$q_v = \frac{Q_T}{V_o}$	2587.5	kJ/m <sup>3</sup>
$Q_{oK} = G_s \cdot q_{oK}$	0.009	kW
$Q_T = Q_1 + Q_{oK}$	0.621	kW
$\eta_m = 0.98 - 0.008 \cdot \frac{P_K}{P_0}$	0.936	-
$\eta_e = 0.97 - 0.02 \cdot \frac{P_K}{P_0}$	0.86	-
$N_v = \frac{N_i}{\eta_m}$	0.17	kW
$N_e = \frac{N_c}{\eta_e \eta_m}$	0.198	kW
$E'_T = \frac{N_c}{Q_T}$	0.31	-
$\Delta N = 0.035 + 0.015 \cdot N_e$	0.03797	kW
$\Delta E_T = \frac{\Delta N}{Q_T}$	0.061	-
$E_T = E'_T + \Delta E_T$	0.371	-
$\mu' = \frac{Q_T}{N_c} = \frac{1}{E'_T}$	3.136	-
$\mu = \frac{Q_T}{N_c + \Delta N} = \frac{1}{E_T}$	2.63	-
$E_c^* = 1 - \frac{T_{n,e}}{T_{in, losses}}$	0.21	-
$\eta'_{m,e} = \frac{E_c^*}{E'_T}$	0.677	-
$\eta_{m,e} = \frac{E_c^*}{E_T}$	0.566	-

In contrast to the energy balance, the exergetic balance considers the degree of technical utility of energy determined by the temperature potential of heat flows [54]. The compressor is provided with two energy sources: supplied electrical energy  $E_e \cdot \eta_m \cdot \eta_e \cdot \eta_u$  and the exergetic flow rate of the sucked working agent  $G_{exe1}$ , exergy of the working agent flow  $G_{flowe2}$  (Table 8).

**Table 8.** Values of refrigerant exergies at characteristic points.

Formula/Method of Determination	Value	Units of Measurement
$E_{total} = N_e + \Delta N$	0.23597	kW
$E_e = N_e$	0.198	kW
$E_m = G_s(e_2 - e_3)$	0.067	kW
$D_{em} = (1 - \eta_m \cdot \eta_e \cdot \eta_u) \cdot E_e$	0.0386	kW
$D_{km} = E_e \cdot \eta_m \cdot \eta_e \cdot \eta_u - G_s(e_2 - e_1)$	0.0119	kW
$T_{in\ losses}^{av} = \frac{T_{in\ losses}'' - T_{in\ losses}'}{\ln \frac{T_{in\ losses}''}{T_{in\ losses}'}}$	371	K
$E_{T1} = Q_T(1 - \frac{T_{n,e}}{T_{c,p}^{BK}})$	0.13	kW
$E_u = G_{xa}(e_4 - e_1)$	0.0495	kW
$D_u = E_u$	0.0495	kW
$E_{o,n} = E_{in,e} \cdot (0.01 \dots 0.03)$	0.00589	kW

The results obtained are summarized in the table of the exergetic balance of the installation (Table 9).

**Table 9.** Exergetic balance of TNU.

Supplied Exergy		Diverted Exergy		
Parish Articles	kW	Expense Items	kW	% κ $E_{total}$
Total electrical power supplied to the installation, including its own needs ( $E_{total}$ )	0.23597	Exergetic heating capacity, $E_{T1}$ :		
		Losses:		
		In the compressor:	0.13	55%
		Electromechanical	0.0386	16%
		Internal	0.0119	5%
		In the evaporator:	0.0495	20%
From the irreversibility of heat exchange own needs	0.00589	2.5%		
Total	0.23597	Total	0.23589	

Next, it is necessary to analyze the calculated components of the balance sheet with an assessment of the efficiency of individual elements and the scheme as a whole, as well as to make recommendations on possible measures to reduce exergy losses in the installation.

*3.3. Future Prospects: Exergetic Method for Evaluating the Efficiency of the Evaporation Plant*

It is necessary to evaluate the efficiency of the evaporation plant. To achieve this goal, the following tasks are solved: determination of enthalpy, entropy, and exergy at characteristic points of the VU cycle, as well as the compilation of the exergetic balance of the VU.

Special attention in the design is paid to the materials from which the equipment is made. Since the unit operates at a high temperature with the deoxidation of water, the body parts of the evaporation chambers are made of carbon steel with a copper–nickel coating. All other structures, including tubes, are made of copper–nickel alloys.

To evaporate water, it is advisable to establish a technological process for obtaining distillate by boiling under a vacuum. For this purpose, a special installation will be used in which two compressors will be involved: one to reduce the pressure in the system, and the other to increase it. The installation also has a coil through which the already heated water will heat the incoming water. The installation works as follows: heated water enters the tank. In this tank, at the first start, the water is heated using an installed heater and the pressure is reduced to discharge. The water temperature practically does not change, but the heat from the heater is used to convert the water into a vaporous form. The

steam then passes through the compressor and the pressure rises, which causes the steam temperature to rise. The steam passing through the coil gives its heat to the water entering the installation and condenses.

The process of thermal distillation has long been a method of desalination to obtain a large amount of fresh water. This is largely due to its technological advantages, such as the simplification of design and construction, and the reliability in operation and automation capabilities [55,56]. In addition, the quality of the produced water meets medical and biological requirements. As a result of adjusting the design of individual elements of the desalination plant, the cost of the water received is steadily decreasing. The classification of modern rectification desalination plants is based on various features, such as the principle of operation, the hydrodynamics of the regime, the method of using the heat of secondary steam, the type of heat-carrier heating surfaces, and the design and method of contact of the heating surface with the liquid. Examples of these features include evaporative and instantaneous boiling, natural and forced circulation of the source water with or without regeneration, steam, gas, and electric heating, tubular and lamellar, vertical and horizontal, single- and multi-row, tower-type, jet-shock, gravity, centrifugal, and swirling currents.

The purpose of creating installations with a thermal process for obtaining fresh water from seawater has led to the development of innovative conceptual and constructive schemes with high efficiency. (Figure 11). Particular attention is paid to the optimization of operating modes, replacement of expensive structural materials, pipe surfaces with other heater configurations, reduction of scale formation with an increase in the initial heating temperature of desalinated water in order to reduce the consumption of thermal and electrical energy to obtain the final product [13]. This goal can be achieved by utilizing low-potential and waste heat. The cost of water obtained in the desalination process is largely determined by the energy source used in the construction of large distilleries.

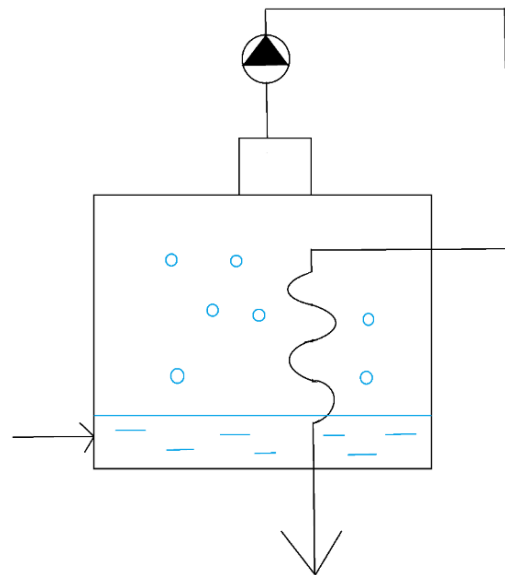


**Figure 11.** Installation diagram.

The distillation process is carried out when its aggregate state changes and is accompanied by the separation into distillate and concentrated solutions [56]. In this case, the change in exergy in such an isobaric–isothermal process takes the form

$$de = \left(1 - \frac{T_0}{T}\right) dq + RT \frac{da}{a} \quad (5)$$

where  $dq$ —The amount of heat supplied (withdrawn);  $a$ —Pure water activity;  $T_0$ —Ambient temperature.

Taking into account phase transformations, the value of exergy

$$e = \int_1^2 \left(1 - \frac{T_0}{T}\right) \cdot c_p dT + \int_2^3 \left(1 - \frac{T_0}{T}\right) \cdot dh + \int_2^3 T \frac{da}{a} \tag{6}$$

The first term characterizes the amount of heat that is needed to heat seawater from ambient temperature to saturation temperature at a constant concentration. If we assume that the heat capacity of water does not depend on concentration and temperature, then

$$\int_T^{T'_S} c_p \left(1 - \frac{T_0}{T}\right) \cdot dT = c_p (T'_S - T_0 - T'_S \ln \frac{T'_S}{T_0}) \tag{7}$$

At the same time, the saturation temperature of the source water

$$T'_S = \frac{T_{S,S}}{r_{S,S} - 2RT_{S,S}^2 b} \tag{8}$$

where  $T_{S,S}$ ,  $r_{S,S}$ —the saturation temperature of the pure solvent and its latent heat of vaporization. At a lower initial concentration of seawater ( $b \sim 20\%$ ), there is a decrease in the exergy spent on heating the solution, since the value of the physico-chemical depression decreases. If we take into account the dependence of the heat capacity on temperature and concentration, then Equation (8) will be reduced to the form

$$\begin{aligned} e_H &= \int_{T_0}^{T'_S} c_p \left(1 - \frac{T_0}{T}\right) \cdot dT = \\ &= A(T'_S - T_0 - T'_S \ln \frac{T'_S}{T_0}) + B(T'^3_S - T_0^3) - C(T'^2_S - T_0^2) + D(T'_S - T_0) - F \ln \frac{T'_S}{T_0} \end{aligned} \tag{9}$$

The energy spent on evaporation will be written as

$$e_H = \int_2^3 \left(1 - \frac{T_0}{T}\right) \cdot dh \approx \frac{1}{2} \left[ \left(1 - \frac{T_0}{T'_S}\right) r'_S + \left(1 + \frac{T_0}{T''_S}\right) r''_S \right] \tag{10}$$

where  $T'_S$ ,  $T''_S$  and  $r'_S$ ,  $r''_S$ —The boiling point and corresponding values of latent heat of vaporization at the initial  $b$  and the final  $b_k$  source water concentrations.

With an increase in the multiplicity of concentration of seawater, an increase in the exergy of  $e_H$  is observed, which can be taken into account by introducing this value into Equation (10):

$$e_H = r_S^0 \left(1 - \frac{T_0 R}{T_{S,S} r_{S,S}} \ln \omega\right) \tag{11}$$

where  $\omega = \frac{b_k}{b}$ —the multiplicity of concentration. Minimum separation work, characterized by the value  $\int_2^3 RT \frac{da}{a}$  calculated from the ratio

$$e_{\min} = -\frac{RT_0}{n_k - n_0} \int_{n_0}^{n_k} \ln a_B \tag{12}$$

This equation is obtained for conditions when the separation process occurs at parameters close to the environment. As shown, for a real installation, it is more rational to calculate by the equation

$$e_{\min} = \frac{\int \int \left\{ 2RT \left[ \frac{c_p(T_{Sp} - T_0) T'_S}{r T_0} \right] b \right\} dT db}{(T'_S - T_0)(b_k - b)} \tag{13}$$

For decades, the energy costs associated with operating thermal desalination plants have been a point of contention for researchers. Despite numerous attempts to reduce energy consumption and the cost of produced water, the consumption of thermal energy

remains high. This is largely due to the main sources of coolant, such as thermal installations, low-pressure steam extraction from turbo generators, and nuclear power plants, which do not significantly improve the efficiency of the thermal distillation process. In addition, the rising cost of fuel has further slowed down progress. Although attempts to use a multi-purpose energy technology complex, including a desalination plant, have yielded some positive results, they have not yet had a significant impact on reducing energy consumption. As fuel prices continue to rise and supplies become increasingly scarce, it is extremely important to explore alternative energy sources and use the heat of secondary energy carriers to heat the source water in the thermal scheme of the desalination plant. Consider the data in Tables 10 and 11.

**Table 10.** Characteristics of water at characteristic points.

Point Number	Pressure $P$ MPa	Temperature		Enthalpy $i$ , kJ/kg	Entropy $s$ , kJ/(kg·K)	Exergy $e$ , kJ/kg
		$t$ , °C	$T$ , K			
At the entrance	0.1	80	353	334.9	1.07	21.9
In capacity	0.047	80	353	340	1.08	24.07
Before the compressor	0.047	82	355	2647	7.62	414.85
After the compressor	0.052	90	363	2662	7.62	429.85
In front of the coil	0.052	82	355	355	1.13	24.42

**Table 11.** Values of specific exergies of the refrigerant at characteristic points.

Point	Value	Units of Measurement
$e = i - T_{n.e} \cdot s - (i_{n.e} - T_{n.e} \cdot S_{n.e})$		
$e_1$	21.9	kJ/kg
$e_2$	24.07	kJ/kg
$e_3$	414.85	kJ/kg
$e_4$	429.85	kJ/kg
$e_5$	24.42	kJ/kg
$\Delta e = e_{i+1} - e_i$		
$\Delta e_{2-1}$	2.17	kJ/kg
$\Delta e_{3-2}$	390.78	kJ/kg
$\Delta e_{4-3}$	15	kJ/kg
$\Delta e_{1-4}$	−405.78	kJ/kg
$\Delta e_{dse} = \sum \Delta e$		
$\Delta e_{dse}$	2.17	kJ/kg

#### 4. Conclusions

1. The main types of heat exchangers and the principles of their operation are considered, as well as modern technologies for increasing their efficiency through design are described. The practical experience of using plate heat exchangers in industry has been studied.

2. An overview is presented on the development of software that is used in the design and optimization of heat exchange devices, as well as improving their energy efficiency. The presented mathematical models can be used for software that is applicable both to individual segments of plates of heat exchangers, as well as to heat exchangers in general, taking into account the dependence of the installation of the entire circuit on environmental parameters and location. In conclusion, recommendations are given for further research directions in the field of using heat exchangers with the inclusion of renewable energy sources.

3. The technique of an energy technology complex, including a heat pump, a photovoltaic panel, and a desalination plant, is presented. The methodology is built around the basic design and energy balance of the complex and is also considered from the point of view of the exergetic balance. This allows for the use of additional components, such as a turbo expander for the implementation of the organic Rankine cycle, a wind turbine, and a solar concentrator. This scientific approach can become unified for the design and operation of an energy technology complex. In addition, an exergetic calculation method is presented for a thermal desalination plant operating as part of an energy technology complex with renewable energy sources.

**Author Contributions:** Conceptualization, K.O., S.A., S.K., T.T., A.K., V.K. and O.K.; Methodology, K.O., S.A., S.K., T.T., A.K. and V.K.; Formal analysis, K.O.; Investigation, K.O.; Data curation, K.O.; Writing—original draft, K.O.; Writing—review & editing, K.O., S.A., S.K., T.T., A.K. and V.K.; Visualization, K.O., S.A., S.K., T.T., A.K. and V.K.; Supervision, K.O.; Project administration, K.O. All authors have read and agreed to the published version of the manuscript.

**Funding:** The study was supported by the Russian Science Foundation Grant No. 22-19-20011, <https://rscf.ru/en/project/22-19-20011/> (accessed on 18 April 2023).

**Data Availability Statement:** There are no data applicable in this study.

**Acknowledgments:** The authors thank South Ural State University (SUSU) for supporting.

**Conflicts of Interest:** The authors declare no conflict of interest.

## Nomenclature

$\varepsilon$	Thermal coefficient of the cycle
$Q_2$	The amount of heat required by the heater
$Q_1$	The amount of heat transferred to water
$T$	Absolute temperature, K
$s = dq/T$	Specific entropy is a thermodynamic parameter of the state, kJ/(kg·K)
$P_1$	Initial freon pressure
$t_1$	Initial temperature of freon
$P_4$	Freon pressure from Table 1
$t_4$	Freon temperature from Table 1
$i_1$	Enthalpy at Point 1
$i_2$	Enthalpy at Point 2
$\eta_{ad}$	Efficiency for freon compressors
$i_a$	Enthalpy at Point A
$T_K$	Condensate temperature
$X_1$	Degree of dryness
$S_{1,2,3}$	Entropy in points
$q_{1,2}$	Specific amount of heat
$h_{1,2,3,4}$	Enthalpy at the corresponding points
$l_{cycle}$	Cycle operation
$e$	Specific exergy
$G$	Expenditure
$Q_{1,2}$	The amount of heat
$i_{n.e.}$	The enthalpy of the environment for a given refrigerant at a temperature of $T_{n.e.}$
$S_{n.e.}$	The entropy of the environment for a given refrigerant at a temperature of $T_{n.e.}$
$T_{n.e.}$	Ambient temperature
$P_{n.e.}$	Pressure at temperature $T_{n.e.}$
$e_{1,2,3,4}$	Values of specific exergies of the refrigerant at characteristic points
$\Delta e_{dse}$	Difference of specific exergies
$V_0$	Expenditure
$q_v$	Specific amount of heat
$N_{v.e.}$	Power
$E_e \cdot \eta_m \cdot \eta_e \cdot \eta_u$	Electrical energy input and efficiency (mechanical, electrical, useful)

$G_{exe1}$	Exergetic consumption of the suction working agent
$G_{flowe2}$	Exergy of the working agent flow
$E$	Exergy
$D$	Media consumption
$E_{h1}$	Exergetic heating capacity
$E_{total}$	Total electrical power supplied to the installation, including its own needs
$a$	Pure water activity
$T_0$	Ambient temperature
$T_{s,s}$	Saturation temperature of the pure solvent
$r_{s,s}$	Its latent heat of vaporization
$T'_S, T''_S$ и $r'_S, r''_S$	Boiling points and corresponding values of latent heat of vaporization at Initial b and Final bk concentrations of source water
$\omega = \frac{b_k}{b}$	The multiplicity of concentration
$E_c^*$	Compressor energy
$T_{in losses}^{av}$	Average value of internal loss temperature
$T'_{in losses}, T''_{in losses}$	Temperature taking into account internal losses at the input and output, respectively
$E_{o.n}$	Energy of own needs
$E_{in.e}$	Supplied energy

#### Acronyms and Abbreviations:

a	Average value
av	Average
c.	Compressor
in losses	Internal losses
in energy	Input energy
o.n.	Own needs
s.s.	Saturated solution
s.	Solution
n.e.	Natural environment
d.s.e.	The difference of specific exergies
a.d.	Adiabata
GHE	Temperature field of the ground heat exchanger
DE	Differential evolution
TDE	Tsallis differential evolution
OCR	Organic Rankine cycle
AT	Average temperature
HT	High temperature
SC	Serial circuit
CC	Condensation circuit
SC/CC	Hybrid scheme
RIR	Return On Investment ratio
WHR	Waste heat recovery
RSC	Rankine steam cycle
PGS	Power generation system
ICE	Internal combustion engine
NCE	Normalized cost of energy
LCA	Life cycle analysis
PCM	Predictive control model
OTC	Organic Transarctic cycle
SC	Supercritical cycle
GT	Gas turbine
RORC	Regenerative organic Rankine Cycle
EF	Efficiency factor
WHR	Waste heat recovery
IHR	Internal heat exchanger

## References

1. Arsenyeva, O.; Tovazhnyansky, L.; Kapustenko, P.; Khavin, G. Mathematical Modelling and Optimal Design of Plate-and-Frame Heat Exchangers. *Chem. Eng. Trans.* **2009**, *18*, 791–796. [[CrossRef](#)]
2. Jiang, C.; Zhou, W.; Tang, X.; Bai, B. Influence of capsule length and width on heat transfer in capsule-type plate heat exchangers. *Adv. Mech. Eng.* **2019**, *11*, 168781401989574. [[CrossRef](#)]
3. Irabatti, V.; Patil, Y.; Kore, S.; Barangule, V.; Kothe, A. Comprehensive review of spiral heat exchanger for diverse applications. *Mater. Today Proc.* **2022**, *72*, 1328–1334. [[CrossRef](#)]
4. Lu, X.; Zhang, G.; Chen, Y.; Wang, Q.; Zeng, M. Effect of geometrical parameters on flow and heat transfer performances in multi-stream spiral-wound heat exchangers. *Appl. Therm. Eng.* **2015**, *89*, 1104–1116. [[CrossRef](#)]
5. Wu, J.; Zhao, J.; Sun, X.; Liu, S.; Wang, M. Design Method and Software Development for the Spiral-Wound Heat Exchanger with Bilateral Phase Change. *Appl. Therm. Eng.* **2019**, *166*, 114674. [[CrossRef](#)]
6. Omid, M.; Farhadi, M.; Jafari, M. A comprehensive review on double pipe heat exchangers. *Appl. Therm. Eng.* **2017**, *110*, 1075–1090. [[CrossRef](#)]
7. Hussein, A. Thermal performance and thermal properties of hybrid nanofluid laminar flow in a double pipe heat exchanger. *Exp. Therm. Fluid Sci.* **2017**, *88*, 37–45. [[CrossRef](#)]
8. Sheikholeslami, M.; Ganji, D.D. Heat transfer improvement in a double pipe heat exchanger by means of perforated turbulators. *Energy Convers. Manag.* **2016**, *127*, 112–123. [[CrossRef](#)]
9. Bezaatpour, M.; Rostamzadeh, H. Heat transfer enhancement of a fin-and-tube compact heat exchanger by employing magnetite ferrofluid flow and an external magnetic field. *Appl. Therm. Eng.* **2019**, *164*, 114462. [[CrossRef](#)]
10. Yanvarev, I.; Grokhotov, V. Multisection heat exchangers for heat utilization of the waste gases from heat power plants. *J. Phys. Conf. Ser.* **2019**, *1260*, 052034. [[CrossRef](#)]
11. Zhurmilova, I.; Shtym, A. Determination of Ground Heat Exchangers Temperature Field in Geothermal Heat Pumps. *IOP Conf. Ser. Mater. Sci. Eng.* **2017**, *262*, 012096. [[CrossRef](#)]
12. Segundo, E.; Amoroso, A.; Mariani, V.; Coelho, L. Economic optimization design for shell-and-tube heat exchangers by a Tsallis differential evolution. *Appl. Therm. Eng.* **2017**, *111*, 143–151. [[CrossRef](#)]
13. Rafalskaya, T.; Rudyak, V. Modeling of characteristics of heat exchangers of heat supply systems in variable operating modes. *J. Phys. Conf. Ser.* **2020**, *1565*, 012005. [[CrossRef](#)]
14. Shaimerdenova, K.M.; Schragger, E.R.; Tussypbaeva, A.S.; Nausharban, Z.K. Investigation of heat exchange processes in vertically arranged heat exchangers. *Bull. Karaganda Univ. Phys. Ser.* **2019**, *94*, 66–72. [[CrossRef](#)]
15. Vescovo, R.; Spagnoli, E. High Temperature ORC Systems. *Energy Procedia* **2017**, *129*, 82–89. [[CrossRef](#)]
16. Teng, S.; Wang, M.; Xi, H.; Wen, S. Energy, exergy, economic (3E) analysis, optimization and comparison of different ORC based CHP systems for waste heat recovery. *Case Stud. Therm. Eng.* **2021**, *28*, 101444. [[CrossRef](#)]
17. Valencia, G.; Isaza-Roldan, C.; Forero, J. Economic and Exergo-Advance Analysis of a Waste Heat Recovery System Based on Regenerative Organic Rankine Cycle under Organic Fluids with Low Global Warming Potential. *Energies* **2020**, *13*, 1317. [[CrossRef](#)]
18. Klimaszewski, P.; Zaniewski, D.; Witanowski, L.; Suchocki, T.; Klonowicz, P.; Lampart, P. A case study of working fluid selection for a small-scale waste heat recovery ORC system. *Arch. Thermodyn.* **2019**, *40*, 159–180. [[CrossRef](#)]
19. Ren, L.; Liu, J.; Wang, H. Thermodynamic Optimization of a Waste Heat Power System under Economic Constraint. *Energies* **2020**, *13*, 3388. [[CrossRef](#)]
20. Cardenas-Gutierrez, J.; Valencia, G.; Duarte-Forero, J. Regenerative Organic Rankine Cycle as Bottoming Cycle of an Industrial Gas Engine: Traditional and Advanced Exergetic Analysis. *Appl. Sci.* **2020**, *10*, 4411. [[CrossRef](#)]
21. Valencia, G.; Cardenas-Gutierrez, J.; Forero, J. Exergy, Economic, and Life-Cycle Assessment of ORC System for Waste Heat Recovery in a Natural Gas Internal Combustion Engine. *Resources* **2020**, *9*, 2. [[CrossRef](#)]
22. Blanco, E.; Valencia, G.; Forero, J. Thermodynamic, Exergy and Environmental Impact Assessment of S-CO<sub>2</sub> Brayton Cycle Coupled with ORC as Bottoming Cycle. *Energies* **2020**, *13*, 2259. [[CrossRef](#)]
23. Shao, Y.; Xiao, H.; Chen, B.; Huang, S.; Qin, F. Comparison and analysis of thermal efficiency and exergy efficiency in energy systems by case study. *Energy Procedia* **2018**, *153*, 161–168. [[CrossRef](#)]
24. Roux, D.; Lalau, Y.; Rebouillat, B.; Neveu, P.; Olives, R. Thermochemical energy storage optimisation combining exergy and life cycle assessment. *Energy Convers. Manag.* **2021**, *248*, 114787. [[CrossRef](#)]
25. James, C.; Kim, T.; Jane, R. A Review of Exergy Based Optimization and Control. *Processes* **2020**, *8*, 364. [[CrossRef](#)]
26. Ren, L.; Wang, H. Optimization and Comparison of Two Combined Cycles Consisting of CO<sub>2</sub> and Organic Trans-Critical Cycle for Waste Heat Recovery. *Energies* **2020**, *13*, 724. [[CrossRef](#)]
27. Tzivanidis, C.; Bellos, E. A Comparative Study of Solar-Driven Trigenation Systems for the Building Sector. *Energies* **2020**, *13*, 2074. [[CrossRef](#)]
28. Zhang, Y.; Zhang, S.; Peng, H.; Tian, Z.; Gao, W.; Yang, K. Thermodynamic analysis of Tesla turbine in Organic Rankine Cycle under two-phase flow conditions. *Energy Convers. Manag.* **2023**, *276*, 116477. [[CrossRef](#)]

29. Gupta, P.; Tiwari, A.; Said, Z. Solar organic Rankine cycle and its poly-generation applications—A review. *Sustain. Energy Technol. Assess.* **2022**, *49*, 101732. [CrossRef]
30. Yağlı, H.; Koç, Y.; Kalay, H. Optimisation and exergy analysis of an organic Rankine cycle (ORC) used as a bottoming cycle in a cogeneration system producing steam and power. *Sustain. Energy Technol. Assess.* **2021**, *44*, 100985. [CrossRef]
31. Koç, Y.; Yağlı, H.; Kalay, I. Energy, Exergy, and Parametric Analysis of Simple and Recuperative Organic Rankine Cycles Using a Gas Turbine–Based Combined Cycle. *J. Energy Eng.* **2020**, *146*, 04020041. [CrossRef]
32. Wang, N.; Zhang, S.; Fei, Z.; Zhang, W.; Shao, L.; Sardari, F. Thermodynamic performance analysis a power and cooling generation system based on geothermal flash, organic Rankine cycles, and ejector refrigeration cycle; application of zeotropic mixtures. *Sustain. Energy Technol. Assess.* **2020**, *40*, 100749. [CrossRef]
33. Qin, N.; Tian, H. Operational analysis of a newly untreated sewage source heat pump with a plate heat exchanger. *Heat Mass Transf.* **2022**, *58*, 683–693. [CrossRef]
34. Bahrami, M.; Pourfayaz, F.; Kasaeian, A. Low global warming potential (GWP) working fluids (WFs) for Organic Rankine Cycle (ORC) applications. *Energy Rep.* **2022**, *8*, 2976–2988. [CrossRef]
35. Popp, T.; Weiß, A.P.; Heberle, F.; Winkler, J.; Scharf, R.; Weith, T.; Brüggemann, D. Experimental Characterization of an Adaptive Supersonic Micro Turbine for Waste Heat Recovery Applications. *Energies* **2021**, *15*, 25. [CrossRef]
36. Bhattad, A.; Sarkar, J.; Ghosh, P. Heat transfer characteristics of plate heat exchanger using hybrid nanofluids: Effect of nanoparticle mixture ratio. *Heat Mass Transf.* **2020**, *56*, 2457–2472. [CrossRef]
37. Bai, Z.; Li, Y.; Zhang, J.; Fewkes, A.; Zhong, H. Research on the design and application of capillary heat exchangers for heat pumps in coastal areas. *Build. Serv. Eng. Res. Technol.* **2021**, *42*, 014362442110014. [CrossRef]
38. Ji, Y.; Wu, W.; Hu, S. Long-term performance of a front-end capillary heat exchanger for a metro source heat pump system. *Appl. Energy* **2023**, *335*, 120772. [CrossRef]
39. Zhao, Y.; Shao, J.; Dai, Y.; Yang, X.; Deng, J. Simulation study on performance of plate heat exchanger for heat pump. *IOP Conf. Ser. Earth Environ. Sci.* **2020**, *608*, 012004. [CrossRef]
40. Mołczan, T.; Cyklis, P. Mathematical Model of Air Dryer Heat Pump Exchangers. *Energies* **2022**, *15*, 7092. [CrossRef]
41. Santa, R. Investigations of the performance of a heat pump with internal heat exchanger. *J. Therm. Anal. Calorim.* **2021**, *147*, 8499–8508. [CrossRef]
42. Perekopnaya, Y.A.; Osintsev, K.V.; Toropov, E.V. Principles of Energy Conversion in Thermal Transformer Based on Renewable Energy Sources. In *Advances in Automation; Lecture Notes in Electrical Engineering*; Radionov, A., Karandaev, A., Eds.; Springer: Cham, Switzerland, 2020; Volume 641. [CrossRef]
43. Osintsev, K.; Aliukov, S. ORC Technology Based on Advanced Li-Br Absorption Refrigerator with Solar Collectors and a Contact Heat Exchanger for Greenhouse Gas Capture. *Sustainability* **2022**, *14*, 5520. [CrossRef]
44. Shishkov, A.N.; Osintsev, K.V. Modernization of technological equipment in the waste water purification process behind the coke oven using the organic Rankine cycle. *IOP Conf. Ser. Mater. Sci. Eng.* **2021**, *1064*, 012032. [CrossRef]
45. Tolstoy, O.V. 2016 Working Substances of the Heat Pump: Advantages and Disadvantages of Priority Scientific Directions in the XXI Century: Materials of the International (Correspondence) Scientific and Practical Conference [Electronic Resource], Prague, Czech Republic, 5 October 2016; Vostretsov, A.I., Ed.; Scientific Publishing Center “World of Science” (IP Vostretsov Alexander Ilyich): Prague, Czech Republic, 2016; pp. 77–80.
46. Drannikov, A.; Tertychnaya, T.; Shevtsov, A.; Zasytkin, N. Generation of alternative energy in the production of bakery products using a heat pump. *Storage Process. Agric. Raw Mater.* **2021**, *83*, 132–145. [CrossRef]
47. Protopopov, K.V.; Zhirebny, I.P.; Garanov, S.A. Methods of regulating the performance of air conditioning units with a heat pump mode News of higher educational institutions. *Mech. Eng.* **2014**, *12*, 76–83.
48. Ian, K.; Pinch, C. *Analysis and Process Integration—A User Guide on Process Integration for the Efficient Use of Energy*, 2nd ed.; Elsevier Ltd.: Amsterdam, The Netherlands, 2007; 415p.
49. Brodyanskiy, V.M.; Fratsher, V.; Michalek, K. *Exergetic Method and Its Applications*; Energoatomizdat: Moscow, Russia, 1988; 288p.
50. Abdelalim, A.; O'Brien, W.; Shi, Z. Development of Sankey Diagrams to Visualize Real HVAC Performance. *Energy Build.* **2017**, *149*, 282–297. [CrossRef]
51. Karaagac, M.O.; Kabul, A.; Ogul, H. First- and second-law thermodynamic analyses of a combined natural gas cyclepower plant: Sankey and Grossman diagrams. *Turk. J. Phys.* **2019**, *43*, 93–108. [CrossRef]
52. Yang, M.H.; Yeh, R.H. Economic performances optimization of the transcritical Rankine Cycle systems in geothermal application. *Energy Convers. Manag.* **2015**, *95*, 20–31. [CrossRef]
53. Javanshir, N.; Mahmoudi, S.; Kordlar, M.A.; Rosen, M.A. Energy and Cost Analysis and Optimization of a Geothermal-Based Cogeneration Cycle Using an Ammonia-Water Solution: Thermodynamic and Thermoeconomic Viewpoints. *Sustainability* **2020**, *12*, 484. [CrossRef]
54. Ostapenko, O.P.; Leshchenko, V.V.; Tikhonenko, R.O. Energy advantages of using steam compression heat pumps with electric and cogeneration drives. *Works VNTU* **2015**. Available online: <https://works.vntu.edu.ua/index.php/works/article/view/437> (accessed on 31 March 2023).

55. Chernyshova, V.A. *Heat Pump and the Rationality of Its Application in the Energy-Saving Complex Priority Areas of Innovation in Industry: A collection of Scientific Articles on the Results of the Eleventh International Scientific Conference, Kazan, 29–30 November 2020*; Limited Liability Company “ENVELOPE”: Kazan, Russia, 2020; Volume Part 1, pp. 256–258.
56. Elistratov, S.L. *Comprehensive Study of the Efficiency of Heat Pumps: Abstract of dis. doct*; Technical Sciences: 01.04.; Publisher eLIBRARY: Novosibirsk, Russia, 2011; 39p.

**Disclaimer/Publisher’s Note:** The statements, opinions and data contained in all publications are solely those of the individual author(s) and contributor(s) and not of MDPI and/or the editor(s). MDPI and/or the editor(s) disclaim responsibility for any injury to people or property resulting from any ideas, methods, instructions or products referred to in the content.